

# Excellence in Chemistry Research

## Announcing our new flagship journal

- Gold Open Access
- Publishing charges waived
- Preprints welcome
- Edited by active scientists



## Meet the Editors of *ChemistryEurope*



**Luisa De Cola**

Università degli Studi  
di Milano Statale, Italy



**Ive Hermans**

University of  
Wisconsin-Madison, USA



**Ken Tanaka**

Tokyo Institute of  
Technology, Japan



# Bismuth Cations: Fluoride Ion Abstraction, Isocyanide Coordination, and Impact of Steric Bulk on Lewis Acidity

Tobias Dunaj,<sup>[a]</sup> Johannes Schwarzmann,<sup>[a]</sup> Jacqueline Ramler,<sup>[a]</sup> Andreas Stoy,<sup>[a]</sup> Sascha Reith,<sup>[a]</sup> Joel Nitzsche,<sup>[a]</sup> Lena Völlinger,<sup>[a]</sup> Carsten von Hänisch,<sup>\*,[a]</sup> and Crispin Lichtenberg<sup>\*,[a]</sup>

**Abstract:** The molecular compound [BiDipp<sub>2</sub>(SbF<sub>6</sub>)], containing the bulky, donor-free bismuth cation [BiDipp<sub>2</sub>]<sup>+</sup> has been synthesized and fully characterized (Dipp = 2,6-*i*-Pr<sub>2</sub>-C<sub>6</sub>H<sub>3</sub>). Using its methyl analog [BiMe<sub>2</sub>(SbF<sub>6</sub>)] as a second reference point, the impact of steric bulk on bismuth-based Lewis acidity was investigated in a combined experimental (Gutmann-Beckett and modified Gutmann-Beckett methods) and

theoretical approach (DFT calculations). Reactivity studies of the bismuth cations towards [PF<sub>6</sub>]<sup>−</sup> and neutral Lewis bases such as isocyanides C≡NR' revealed facile fluoride ion abstraction and straightforward Lewis pair formation, respectively. The first examples of compounds featuring bismuth-bound isocyanides have been isolated and fully characterized.

## Introduction

The transformation of neutral bismuth species into cationic congeners has granted access to compounds featuring remarkable structural properties and reactivity patterns.<sup>[1]</sup> This includes low-coordinate and low-valent compounds (such as [Bi(2,6-Mes<sub>2</sub>C<sub>6</sub>H<sub>3</sub>)<sub>2</sub>][B(3,5-(CF<sub>3</sub>)<sub>2</sub>-C<sub>6</sub>H<sub>3</sub>)<sub>4</sub>] (Mes = 2,4,6-Me<sub>3</sub>C<sub>6</sub>H<sub>2</sub>) and [Bi(cAAC)<sub>2</sub>][OTf)],<sup>[2,3]</sup> species with an unusual coordination chemistry (such as a pentagonal bipyramidal coordination geometry with a stereochemically inactive lone pair at bismuth),<sup>[4]</sup> ring-strained coordination entities,<sup>[5–7]</sup> and new structural motifs such as bisma-alkene species and Bi→Bi donor-acceptor bonding.<sup>[8,9]</sup> It can be anticipated that such uncommon structural properties inevitably lead to unforeseen reactivity patterns. Remarkable examples include CH activation reactions,<sup>[5,7,6]</sup> the activation of small molecules such as CO,<sup>[10a]</sup> reversible one-electron transfer at bismuth,<sup>[10,11]</sup> the controlled living radical polymerization of activated  $\alpha$ -olefins,<sup>[12]</sup> the catalytic hydrosilylation of olefins and carbonyl compounds,<sup>[13,14]</sup> and the exploitation of bismuth redox platforms in the fluorination, triflation, and nonaflation of arylboronic esters.<sup>[15,45]</sup>

These findings initiated investigations towards a more detailed understanding of bismuth-based Lewis acidity. As a result, the ability of bismuth(III) species to adopt formal charges ranging from +1 to +3,<sup>[1,9,13,14,16]</sup> to bear multiple Lewis acidic binding sites that can reversibly be occupied by Lewis bases,<sup>[13]</sup> and to act as exceptionally strong and soft Lewis acids has been uncovered.<sup>[17]</sup> Smart ligand design including the use of chelating ligands and the control of the ligand bite angle can be exploited to significantly increase the Lewis acidity of bismuth cations.<sup>[18,19]</sup> In addition, facets such as inversed solvent effects (where the increase of the solvent polarity increases the Lewis acidity) have been reported.<sup>[4]</sup> The use of steric bulk for the stabilization of cationic bismuth species is well documented.<sup>[11]</sup> However, the impact of steric factors on the Lewis acidity of bismuth cations has not been investigated in detail, quantified, and rationalized to so far.

While often receiving less attention, the choice of the counteranion can also be a decisive factor in the design of cationic species, since they can considerably influence the solubility, coordination number, and stability of the cationic species.<sup>[20]</sup> However, the stability and potential degradation pathways of weakly coordinating anions in the coordination sphere of bismuth cations has only received little attention to date.<sup>[21]</sup>

Here, we report the investigation of compounds featuring the structural motif [BiR<sub>2</sub>]<sup>+</sup> (R = Me, Dipp), evaluating steric factors, the stability of [PnF<sub>6</sub>]<sup>−</sup> anions (Pn = P, Sb), and the coordination of Lewis bases in the context of bismuth-based Lewis acidity.

## Results and Discussion

In past experiments, donor-free [BiMe<sub>2</sub>(SbF<sub>6</sub>)] (I) was successfully synthesized.<sup>[8]</sup> In this report, we want to prepare donor-free bismuthenium cations with larger aryl substituents to inves-

[a] T. Dunaj, J. Schwarzmann, Dr. J. Ramler, Dr. A. Stoy, S. Reith, J. Nitzsche, L. Völlinger, Prof. Dr. C. von Hänisch, Prof. Dr. C. Lichtenberg  
Fachbereich Chemie, Philipps Universität Marburg  
Hans-Meerwein-Straße 4, 35043 Marburg (Germany)  
E-mail: carsten.vonhaenisch@chemie.uni-marburg.de  
crispin.lichtenberg@chemie.uni-marburg.de

Supporting information for this article is available on the WWW under <https://doi.org/10.1002/chem.202204012>

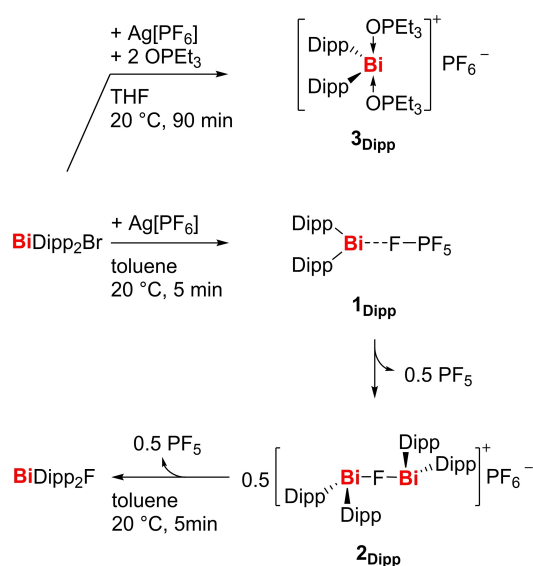
Part of a Special Collection on the p-block elements.

© 2023 The Authors. Chemistry - A European Journal published by Wiley-VCH GmbH. This is an open access article under the terms of the Creative Commons Attribution Non-Commercial NoDerivs License, which permits use and distribution in any medium, provided the original work is properly cited, the use is non-commercial and no modifications or adaptations are made.

tigate the influence of electronic and steric effects of an intermediate-sized aryl substituent on the properties of the bismuthenium atoms. A compound with large terphenyl substituents, has previously been reported in the literature ( $[\text{Bi}((2,6\text{-Mes-C}_6\text{H}_3)_2)[\text{B}(3,5\text{-(CF}_3)_2\text{C}_6\text{H}_3)_4]]$ ).<sup>[2]</sup> However, due to the extreme steric demand of the terphenyl substituent, the crowded bismuth center may not be suitable as a Lewis acid towards donors of considerable size. As a result,  $[\text{BiDipp}_2]^+$  was chosen as the target cation (Dipp = 2,6-*i*-Pr<sub>2</sub>-C<sub>6</sub>H<sub>3</sub>). In first attempts  $\text{BiDipp}_2\text{Br}$  was reacted with  $\text{Ag}[\text{PF}_6]$  in toluene. Upon addition of the silver salt, the reaction mixture immediately turns dark red, indicating the possible formation of the desired  $[\text{BiDipp}_2(\text{PF}_6)]$  (**1**<sub>Dipp</sub>). Upon fast workup, a dark red solid can be obtained. The crude product supposedly consists mainly of **1**<sub>Dipp</sub>, however upon attempted purification or storage under inert atmosphere, the solid decomposes to an inhomogeneous mixture of black and yellow color over few a days. If the reaction mixture is not worked up fast enough, slow precipitation of an orange solid is observed. The orange precipitate represents a mixture of compounds, none of which could be isolated so far. However,  $[(\text{BiDipp}_2)_2\text{F}(\text{PF}_6)]$  (**2**<sub>Dipp</sub>) and literature-known  $\text{BiDipp}_2\text{F}$  could be identified by single-crystal X-ray analysis and NMR spectroscopy, respectively. Thus, we suggest the initial formation of short-lived  $[\text{BiDipp}_2(\text{PF}_6)]$  (**1**<sub>Dipp</sub>), which readily decomposes through a stepwise and facile fluoride ion abstraction from  $[\text{PF}_6]^-$  (Scheme 1, bottom). The formation of  $\text{PF}_5$  was confirmed by NMR spectroscopy after condensation of volatiles from a reaction mixture of  $\text{BiDipp}_2\text{Br}$  and  $\text{Ag}[\text{PF}_6]$  onto an excess of DMAP (Supp. Inf.). The structural analysis of **2**<sub>Dipp</sub> reveals two crystallographically distinct molecules in the solid state. While the Bi–F bond lengths in these molecules are similar to each other and in the range of 2.275(4)–2.296(4) Å, the Bi–F–Bi angle varies dramatically, indicating a bent geometry in one case (144.0(2)°) and a linear coordination in

the other (180°, F atom located on an inversion center). This is a rare case of an organobismuth(III) compound with a bridging fluoro ligand (cf,  $[\text{Bi}(\text{C}_2\text{F}_5)_2\text{F}(\text{OCMe}_2)]_\infty$ , Bi–F–Bi, 138°)<sup>[22]</sup> and demonstrates that the linear and bent arrangements are similar in energy. This is confirmed by DFT calculations which revealed a bent (Bi–F–Bi, 158.3°) and a linear (Bi–F–Bi, 176.0°) isomer of the  $[\text{Dipp}_2\text{Bi–F–BiDipp}_2]^+$  cation as minima on the potential energy surface, the bent species being marginally lower in energy ( $\Delta H = -1.5 \text{ kcal}\cdot\text{mol}^{-1}$ ;  $\Delta G = -2.4 \text{ kcal}\cdot\text{mol}^{-1}$ ). This parallels previous findings in bismuth(V) and mixed bismuth(III/V) chemistry.<sup>[23,24]</sup> In a similar reaction,  $\text{Me}_2\text{BiCl}$  (**II**) was reacted with  $\text{Ag}[\text{PF}_6]$  in toluene, which gave a complex mixture of products according to <sup>1</sup>H and <sup>19</sup>F NMR spectroscopy, none of which could unambiguously be identified. While bismuth cations with neutral donor ligands and  $[\text{PF}_6]^-$  counteranions such as  $[\text{BiPh}_2(\text{NC}_5\text{H}_5)_2]^+$  are accessible,<sup>[25]</sup> our results indicate that  $[\text{PF}_6]^-$  is not a suitable anion for the preparation of donor-free organobismuth cations. These experimental findings are in line with previously reported theoretical calculations, which assigned a fluoride ion affinity (FIA) of 602 to  $[\text{Bi}(2,6\text{-Mes}_2\text{C}_6\text{H}_3)_2]^+$  (level of theory: B3PW91/6-311 + G(2df,p)),<sup>[26]</sup> surpassing the FIA of 384 found for  $\text{PF}_5$  (level of theory: DLPNO-CCSD(T)/aug-cc-pVQZ).<sup>[27]</sup>

In order to obtain indications of the *in situ*-formation of **1**<sub>Dipp</sub> in solution we attempted to trap reactive intermediates with  $\text{OPET}_3$ , which subsequently yielded  $[\text{BiDipp}_2(\text{OPET}_3)_2][\text{PF}_6]$  (**3**<sub>Dipp</sub>) as a colorless crystalline solid. Crystals suitable for single-crystal X-ray diffraction were obtained from a mixture of toluene and *n*-pentane at –32 °C (Figure 1). In **3**<sub>Dipp</sub>, the bismuth atom shows a bisphenoidal coordination geometry with an O–Bi–O angle of 165.84(7)°. The Bi–O bond lengths of 2.4389(16) and 2.4357(16) Å are slightly longer than those in similar Bi<sup>III</sup> phosphanoxide adducts of the general form  $[\text{BiAr}_2(\text{OPR}_3)_2][\text{A}]$  (Ar = Ph, Mes; R = Ph, NMe<sub>2</sub>;  $[\text{A}]^- = [\text{BF}_4]^-$ ,  $[\text{PF}_6]^-$ ; Bi–O, 2.317(5) Å–2.41(1) Å).<sup>[25]</sup> The Bi–O bond elongation in **3**<sub>Dipp</sub> was assigned to the sterically demanding Dipp substituents.



**Scheme 1.** Reaction of  $\text{Dipp}_2\text{BiBr}$  and  $\text{Ag}[\text{PF}_6]$  with **1**<sub>Dipp</sub> and subsequent fluoride transfer from  $[\text{PF}_6]^-$  with formation of **2**<sub>Dipp</sub> and  $\text{BiDipp}_2\text{F}$ . In the presence of  $\text{OPET}_3$ ,  $\text{BiDipp}_2\text{Br}$  reacts with  $\text{Ag}[\text{PF}_6]$  to form **3**<sub>Dipp</sub>.

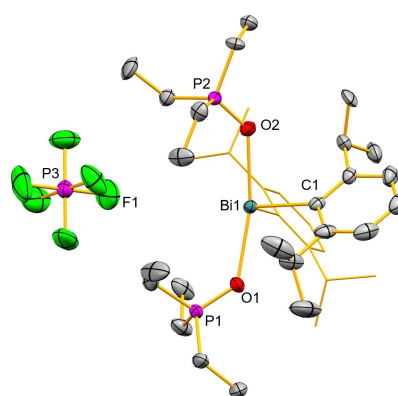
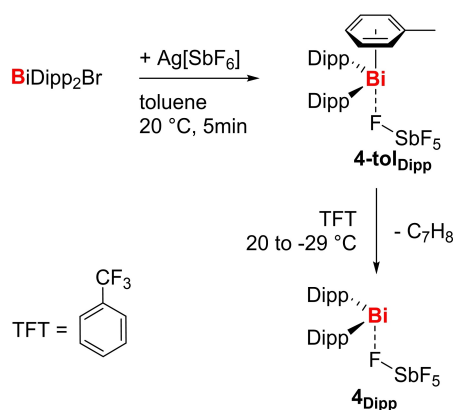


**Figure 1.** Molecular structure of **3**<sub>Dipp</sub> in the solid state. Displacement ellipsoids are drawn at the 50 % probability level. H atoms are omitted and one of the Dipp ligands is shown as wireframe for clarity. Selected bond lengths [Å] and angles [°]: Bi1–O1 2.4359(16), Bi1–O2 2.4389(16), Bi–C1 2.285(2), Bi–C2 2.326(5), O1–Bi1–O2 165.84(7), C1–Bi1–C2 92.3(2), C1–Bi1–O1 104.37(8), C1–Bi1–O2 88.12(8).

To obtain the donor-free  $[\text{BiDipp}_2]^+$  cation, we exchanged the  $[\text{PF}_6]^-$  anion for  $[\text{SbF}_6]^-$ , which already proved to be a suitable strategy in the preparation of  $[\text{BiMe}_2(\text{SbF}_6)]$ .<sup>[8]</sup> Upon addition of  $\text{Ag}[\text{SbF}_6]$  to a toluene solution of  $\text{BiDipp}_2\text{Br}$ , the reaction mixture turned dark red. After removal of solids, concentration and storage at  $-32^\circ\text{C}$ , dark red crystals were obtained and identified as  $[\text{BiDipp}_2(\text{tol})(\text{SbF}_6)]$  (**4-tol<sub>Dipp</sub>**; Scheme 2). For the  $[\text{SbF}_6]^-$  anion, no hints for fluoride abstraction could be observed, indicating that the FIA of the  $[\text{BiDipp}_2]^+$  cation in toluene solution lays in between those of  $\text{PF}_5$  (384) and  $\text{SbF}_5$  (496).<sup>[27]</sup>

Compound **4-tol<sub>Dipp</sub>** crystallizes in the monoclinic space group  $P2_1$ , forming a monomeric ion pair in the solid state (Figure 2). The Bi atom shows a bisphenoidal coordination sphere with two Dipp substituents in the equatorial positions, an  $\eta^6$ -coordinated toluene molecule, and the  $[\text{SbF}_6]^-$  anion coordinated *via* one fluorine atom. The distance of the Bi atom and the centroid of the aromatic toluene ring is 3.2301(3) Å, which is in the range of bonding Bi-arene  $\pi$ -interactions<sup>[28]</sup> and similar to the Bi-*ct* distances in  $\text{BiCl}_3 \cdot \text{C}_6\text{H}_5\text{Me}$  (3.04 and 3.09 Å)<sup>[29]</sup> or  $[\text{Bi}(\text{NMe}_2)_2(\text{BPh}_4)]$  (3.228(5) Å).<sup>[21]</sup> The Bi–F1 distance of 2.488(5) Å is far below the sum of van der Waals radii



**Scheme 2.** Reaction of  $\text{BiDipp}_2\text{Br}$  and  $\text{Ag}[\text{SbF}_6]$  in toluene with formation of **4-tol<sub>Dipp</sub>** and subsequent recrystallization from TFT ( $\alpha, \alpha, \alpha$ -trifluorotoluene) to the donor-free **4Dipp**.

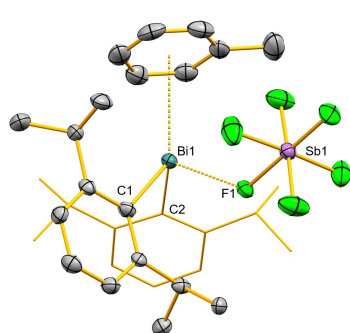


**Figure 2.** Crystal structure of **4-tol<sub>Dipp</sub>** with displacement ellipsoids drawn at the 50% probability level, H atoms are omitted, and one of the Dipp ligands is shown as wireframe for clarity. Selected bond lengths [Å] and angles [ $^\circ$ ]: Bi1–C1 2.259(8), Bi1–C2 2.257(7), Bi1–*ct* 3.2301(3), Bi–F1 2.491(4), Sb1–F1 1.918(6), C1–Bi1–C2 94.4(3), C1–Bi1–F1 86.6(2), C2–Bi1–F1 104.1(2).

(3.54 Å),<sup>[30,31]</sup> similar to that in cation  $[\text{BiMe}_2(\text{SbF}_6)]$  (**I**) (2.451(3) and 2.452(3) Å),<sup>[8]</sup> and significantly longer than that in neutral  $\text{BiDipp}_2\text{F}$  (2.115(3) Å).<sup>[32]</sup> In return, the Sb1–F1 bond in **4-tol<sub>Dipp</sub>** (1.930(7) Å) is elongated compared to the other Sb–F bonds (1.851(7)–1.871(6) Å).

The donor free compound **4Dipp** was obtained by recrystallization of **4-tol<sub>Dipp</sub>** from a less  $\pi$ -donating aromatic solvent, namely  $\alpha, \alpha, \alpha$ -trifluorotoluene (TFT). Compound **4Dipp** crystallizes in the monoclinic space group  $P2_1/n$  with one molecule in the asymmetric unit (Figure 3). In the solid state, dimers are formed through weak interactions of Bi and an F atom of the  $[\text{SbF}_6]^-$  anion in the neighboring molecule, which corresponds to a decrease in nuclearity when compared to the parent compound  $[\text{BiMe}_2(\text{SbF}_6)]_\infty$  (**II**)<sub>∞</sub> that forms a coordination polymer with weakly bound  $\mu_2$ -( $\text{SbF}_6$ )<sup>−</sup> bridging ligands in the solid state. As a result, the bismuth atom in **4Dipp** shows a bisphenoidal coordination sphere with one short Bi1...F1 distance of 2.459(2) Å, similar to that in **4-tol<sub>Dipp</sub>**, and a longer Bi1...F2' distance of 3.208(2) Å, the latter being 9% under the sum of the van der Waals radii (3.54 Å).<sup>[30,31]</sup> The compounds **4Dipp** and **4-tol<sub>Dipp</sub>** show all expected signals in the  $^1\text{H}$  and  $^{13}\text{C}$  NMR spectra, with equal chemical shifts in  $\text{CD}_2\text{Cl}_2$  or  $\text{C}_6\text{D}_6$ , indicating no coordination of the toluene molecule in solution. As obtaining **4-tol<sub>Dipp</sub>** requires less steps while showing the same behavior in solution as **4Dipp**, the former was used for most subsequent reactions. For compounds of the form  $\text{BiDipp}_2\text{X}$  ( $\text{X} = \text{I}, \text{Br}, \text{Cl}, \text{F}, \text{OTf}$ ), the NMR chemical shift of the bismuth-bound carbon atoms could be correlated to the group electronegativity of X, and a low-field shift from 174.5 ( $\text{X} = \text{I}$ ) to 207.6 ( $\text{X} = \text{OTf}$ ) was observed.<sup>[32]</sup> In case of **4Dipp**, a chemical shift of 238.1 ppm ( $\text{C}_6\text{D}_6$ ) or 237.6 ( $\text{CD}_2\text{Cl}_2$ ) is observed, corresponding to an even lower field. In the  $^{19}\text{F}$  NMR spectrum, a very broad signal at 120.8 ppm ( $\text{C}_6\text{D}_6$ ) or 122.9 ( $\text{CD}_2\text{Cl}_2$ ) is observed, hinting at the formation of a contact-ion pair in solution (Figures S3, S16, and S19).

As **2Dipp** was not isolable due to decomposition of the  $[\text{PF}_6]^-$  anion, we attempted to reproduce the  $[(\text{BiDipp}_2)_2\text{F}]^+$  structural motif with an  $[\text{SbF}_6]^-$  anion. Upon reaction of **4-tol<sub>Dipp</sub>** with  $\text{BiDipp}_2\text{F}$  in toluene,  $[(\text{BiDipp}_2)_2\text{F}(\text{SbF}_6)]$  (**5Dipp**) precipitates as an orange

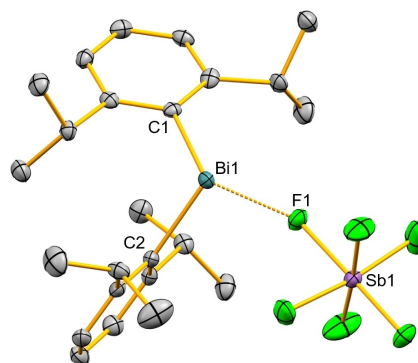
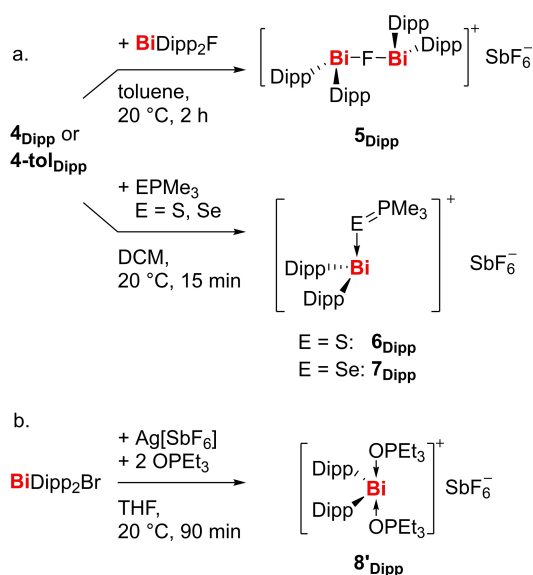


**Figure 3.** Crystal structure of **4Dipp** with displacement ellipsoids drawn at the 50% probability level, H atoms are omitted for clarity. Selected bond lengths [Å] and angles [ $^\circ$ ]: Bi1–C1 2.257(2), Bi1–C2 2.260(2), Bi–F1 2.4593(15), Sb1–F1 1.9438(14), C1–Bi1–C2 97.86(9), C1–Bi1–F1 103.61(7), C2–Bi1–F1 91.19(7).

solid (Scheme 3). Compound **5<sub>Dipp</sub>** crystallizes in the triclinic space group  $P\bar{1}$  with half a molecule of **5<sub>Dipp</sub>** in the asymmetric unit. The central fluorine atom and the antimony atom of the  $[\text{SbF}_6]^-$  anion occupy inversion centers in the unit cell (Figure 4), which results in a perfectly linear coordination of the fluorine atom. Only recently, cationic  $\text{Bi}^{\text{V}}$  compounds with a bridging fluoride motif have been isolated,<sup>[23]</sup> one of them,  $[(\text{BiF}(\text{m-tBu}_2\text{C}_6\text{H}_3)_2)_2\text{F}][\text{B}(\text{3,5-(CF}_3)_2\text{C}_6\text{H}_3)_4]$ , also showing a linearly coordinated fluorine atom. However, **5<sub>Dipp</sub>** is the first isolated cationic dinuclear  $\text{Bi}^{\text{III}}$  compound with a bridging  $\text{F}^-$  anion and can be viewed as a structural excerpt of the one dimensional polymeric chains formed by  $\text{BiDipp}_2\text{F}$  in the solid state.<sup>[32]</sup> The Bi1-F1 distance of 2.2755(4) Å in **5<sub>Dipp</sub>** is somewhat longer than that in the neutral compounds  $\text{BiDipp}_2\text{F}$  (2.115(3) Å)<sup>[32]</sup> or  $\text{Bi}(\text{C}_2\text{F}_5)_2\text{F}$ -acetone (2.229(2) and 2.262(2) Å)<sup>[22]</sup> and very similar to that in the dinuclear  $\text{Bi}^{\text{V}}$  compound described by Cornella and co-workers (2.2820(3) Å).<sup>[23]</sup> Again, there are weak directional

bonding interactions between the bismuth cation and the anion in the solid state (according to distance criteria), and the Bi1...F2 distance of 2.872(4) Å is clearly below the sum of van der Waals radii (3.54 Å).<sup>[30,31]</sup>

The above findings have allowed to grossly map the fluoride ion affinity of  $(\text{BiDipp}_2)^+$  in the condensed phase, which represents one measure of Lewis acidity. To further experimentally explore the Lewis acidity of this species, we aimed to use the Gutmann Beckett method (GBM), which is based on the determination of the  $^{31}\text{P}$  NMR chemical shift of coordinated  $\text{OPET}_3$ . Recently, we proposed a Lewis acidity scale which uses the softer donors  $\text{SPMe}_3$  or  $\text{SePMe}_3$  as probes while otherwise relying on the same principles as the GBM, thereby creating a possibility to evaluate the softness and strength of Lewis acids.<sup>[17,33,34]</sup> Along these lines, **4-tol<sub>Dipp</sub>** was reacted with  $\text{EPMe}_3$  ( $\text{E}=\text{S}, \text{Se}$ ) to give  $[\text{BiDipp}_2(\text{EPMe}_3)(\text{SbF}_6)]$  ( $\text{E}=\text{S}$  (**6<sub>Dipp</sub>**),  $\text{E}=\text{Se}$  (**7<sub>Dipp</sub>**)) in good yields of 92% (**6<sub>Dipp</sub>**) and 59% (**7<sub>Dipp</sub>**). Moreover, the preparation of the mono- $\text{OPET}_3$ -adduct  $[\text{BiDipp}_2(\text{OPET}_3)(\text{SbF}_6)]$  (**8<sub>Dipp</sub>**) was attempted for an evaluation by the original GBM, but only the bis- $\text{OPET}_3$  adduct  $[\text{BiDipp}_2(\text{OPET}_3)_2(\text{SbF}_6)]$  (**8'<sub>Dipp</sub>**) could be isolated (for a more detailed discussion, see DFT section). The compounds **6<sub>Dipp</sub>** and **7<sub>Dipp</sub>** crystallize isomorphically in the space group  $P2_1/c$  with one molecule in the asymmetric unit (Figure 5). The Bi1–S1 bond length in **6<sub>Dipp</sub>** is 2.6700(8) Å, only slightly longer than that in neutral diaryl bismuth sulfides  $(\text{Ar}_2\text{Bi})_2\text{S}_n$  ( $\text{Ar}=\text{Mes}, \text{Dipp}; n=1, 3, 5$ ): 2.520(7)–2.601(2) Å;  $\text{Ph}_2\text{Bi} \cdots \text{SPh}$ : 2.588(1) Å,<sup>[32,35]</sup> and close to that in  $[\text{Bi}(\text{aryl})_2(\text{SPMe}_3)][\text{SbF}_6]$  (2.611(2) Å), where a DFT study and NBO analysis suggested the interpretation of the Bi–S interaction as a regular covalent bond.<sup>[17]</sup> An analogous situation is found for compound **7<sub>Dipp</sub>** (Bi1–Se1, 2.7687(5) Å), when compared to the previously reported compound  $[\text{Bi}(\text{aryl})_2(\text{SePMe}_3)][\text{SbF}_6]$  (Bi–Se, 2.7222(4) Å).<sup>[17]</sup> The F atoms in the  $[\text{SbF}_6]^-$  anion are disordered with an occupancy of 49% and 51% for **6<sub>Dipp</sub>** and 54% and 46% for the two domains in **7<sub>Dipp</sub>**. The shortest Bi–F distance in **6<sub>Dipp</sub>** is 3.132(7) Å and similarly 3.180(4) Å in **7<sub>Dipp</sub>**. This is only slightly shorter than the



**Scheme 3.** a) Preparation of **5<sub>Dipp</sub>**, **6<sub>Dipp</sub>** and **7<sub>Dipp</sub>** from **4-tol<sub>Dipp</sub>** or **4<sub>Dipp</sub>**. b) Preparation of **8'<sub>Dipp</sub>**.

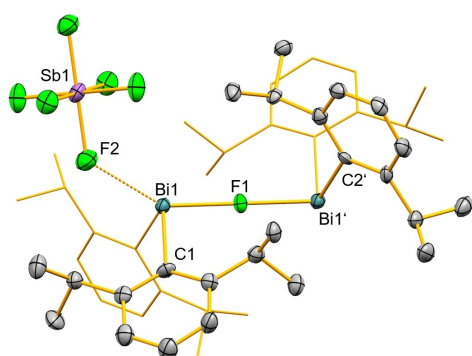


**Figure 4.** Crystal structure of **5<sub>Dipp</sub>** with displacement ellipsoids drawn at the 50% probability level, H atoms are omitted and the second Dipp shown as wireframe for clarity. Selected bond lengths [Å] and angles [°]: Bi–C1 2.287(6), Bi–C2 2.285(6), Bi1–F1 2.2755(4), C1–Bi1–C2 96.0(2), C1–Bi1–F1 101.65(16), C2–Bi1–F1 93.17(16).

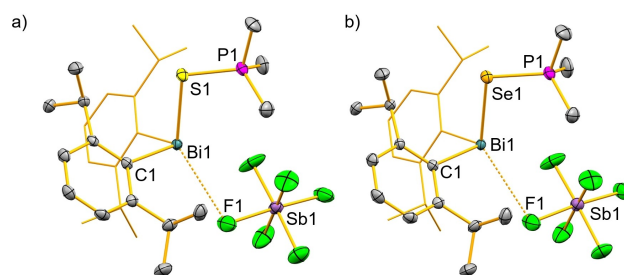


**Figure 5.** Crystal structure of **6<sub>Dipp</sub>** and **7<sub>Dipp</sub>** with displacement ellipsoids drawn at the 50% probability level, H atoms are omitted and the second Dipp is shown as wireframe for clarity. a) Selected bond lengths [Å] and angles [°] of **6<sub>Dipp</sub>**: Bi1–S1 2.6699(7), Bi1–C1 2.277(3), Bi1–C2 2.287(3), S1–P1 2.022(1), C1–Bi1–C2 95.87(9), C1–Bi1–S1 90.02(7), C2–Bi1–S1 106.13(7), Bi1–S1–P1 99.09(4). b) Selected bond lengths [Å] and angles [°] of **7<sub>Dipp</sub>**: Bi1–Se1 2.7689(2), Bi1–C1 2.283(2), Bi1–C2 2.289(2), Se1–P1 2.1755(7), C1–Bi1–C2 95.90(8), C1–Bi1–Se1 89.85(5), C2–Bi1–Se1 106.63(6), Bi1–S1–P1 95.65(2).

intermolecular contact in  $4_{\text{Dipp}}$  (3.208(2) Å) and indicative of weak Bi–F interactions.

In order to evaluate the impact of steric factors on bismuth-based Lewis acidity, the Gutmann-Beckett method and modified versions thereof were applied to compound  $[\text{BiDipp}_2(\text{SbF}_6)]$  ( $4_{\text{Dipp}}$ ) with its bulky Dipp ligands and compound  $[\text{BiMe}_2(\text{SbF}_6)]$  (**I**) bearing methyl groups, that is, ligands with a very low steric profile. Acceptor numbers (AN) for  $4_{\text{Dipp}}$  and  $[\text{BiMe}_2(\text{SbF}_6)]$  (**I**) were determined through the  $^{31}\text{P}$  NMR shifts obtained from the analysis of isolated compounds or from *in situ* experiments and calculated according to formulae (1) to (3) for the respective donor.<sup>[17,33,34]</sup>

$$\text{OPeT}_3 : \text{AN} = 2.21 (\delta_{\text{p}} - 41.0) \quad (1)$$

$$\text{SPMe}_3 : \text{AN} = 6.41 (\delta_{\text{p}} - 29.2) \quad (2)$$

$$\text{SePMe}_3 : \text{AN} = 5.71 (\delta_{\text{p}} - 7.8) \quad (3)$$

While the limitations and the theoretical background of the Gutmann Beckett method have been discussed on a few instances, the method still provides an experimental evaluation of Lewis acidity in a straightforward approach without the necessity for a special experimental setup.<sup>[17,36]</sup> According to the Gutmann-Beckett approach, low acceptor numbers are caused by weak interactions between the donor ( $\text{OPeT}_3$ ,  $\text{SPMe}_3$ ,  $\text{SePMe}_3$ ) and the acceptor and indicate a low Lewis acidity. On the other hand, high acceptor numbers are the result of stronger interactions between the donor and the acceptor, indicating a higher Lewis acidity. The results obtained for  $[\text{BiDipp}_2(\text{SbF}_6)]$  ( $4_{\text{Dipp}}$ ) and  $[\text{BiMe}_2(\text{SbF}_6)]$  (**I**) are summarized in Table 1. In order to compare the ability of these compounds to bind not only one but two donors, experiments with two equivalents of the Lewis base were also performed. As a trend, the acceptor numbers of compound  $4_{\text{Dipp}}$  are greater than those of **I** (with a few exceptions where similar acceptor numbers were determined). Thus, the increase of steric bulk increases rather than decreases the Lewis acidity. Electronic effects seem to play a minor role in these particular cases, since the acceptor numbers of species based on the complex fragment  $[\text{BiPh}_2]^+$  have been reported to be similar to those of **I**.<sup>[17,37]</sup> The most prominent difference between **I** and  $4_{\text{Dipp}}$  is found for the Lewis acidity

towards  $\text{OPeT}_3$  (entries 1, 2), where **I** gives results that are in line with previous findings,<sup>[6,17,18,37]</sup> but  $4_{\text{Dipp}}$  shows a very pronounced Lewis acidity that even surpasses that of a tri-cationic bismuth species<sup>[19]</sup> and bismuth cations, in which the Lewis acidity has been increased by tuning of the ligand bite angle.<sup>[18]</sup> While acceptor numbers in experiments with two equivalents of a donor are expectedly smaller than in cases of a 1:1 stoichiometry, these results indicate that the simultaneous and considerable activation of two Lewis bases at the bismuth centers of  $4_{\text{Dipp}}$  and **I** is possible.

To further elucidate the Lewis acidic properties of compounds  $[\text{BiR}_2(\text{SbF}_6)]$  ( $\text{R} = \text{Me}$ , Dipp), DFT calculations were performed at the B3LYP/6-311++G(d,p) [H,C,O,F,P,S,Se] LanL2DZ [Sb,Bi] level of theory using the D3 version of Grimme's dispersion model (for details see the Supporting Information). The most striking difference between the Gutmann-Beckett parameters of these compounds is the higher Lewis acidity of the sterically more demanding species towards one equivalent of  $\text{OPeT}_3$  (Table 1, entries 1, 2, see Discussion above). The geometry-optimized structures of  $[\text{BiR}_2(\text{OPeT}_3)(\text{SbF}_6)]$  ( $\text{R} = \text{Me}$ , Dipp) revealed that the bulky Dipp substituents effectively shield the bismuth atom, resulting in a solvent-separated ion pair, while a contact ion pair is formed for the compound featuring a  $\text{BiMe}_2^+$  core (Figure 6). Thus, the lower coordination number as such and the absence of a weakly bound ligand in the *trans* position to the spectroscopic probe  $\text{OPeT}_3$  result in a significantly higher acceptor number for  $8_{\text{Dipp}}$ . The addition of the first and the second equivalent of  $\text{EPR}'_3$  ( $\text{E} = \text{O}$ , S, Se;  $\text{R}' = \text{Me}$ , Et) to  $[\text{BiR}_2(\text{SbF}_6)]$  ( $\text{R} = \text{Me}$  (**I**), Dipp ( $4_{\text{Dipp}}$ )) is exothermic and exergonic in all reactions that were studied (Table 2). Thus, the formation of compounds  $[\text{BiR}_2(\text{EPR}'_3)_2(\text{SbF}_6)]$  can be expected in all cases, when two equivalents of the base are present. A more detailed analysis reveals that the energy gain in the second addition is larger for the compounds with the  $\text{BiMe}_2^+$  core (entries 3, 6, 9) than for those with a  $\text{BiDipp}_2^+$  core (entries 12, 15, 18), which was ascribed to the absence of strong steric repulsion in the former cases. When studying the trends of the energy gain for the addition of the second equivalent of a Lewis base in the  $\text{BiMe}_2^+$  and  $\text{BiDipp}_2^+$  series (entries 3, 6, 9 and 12, 15, 18), it is relatively small for the softer Lewis bases S/SePMe<sub>3</sub> in the compounds

**Table 1.** Acceptor numbers (ANs) of compounds  $[\text{BiR}_2(\text{SbF}_6)]$  ( $\text{R} = \text{Me}$ , Dipp) according to the Gutmann-Beckett method and variations thereof.

	Donor	Eq.	Acceptor	AN
1	$\text{OPeT}_3$	1	$[\text{BiMe}_2(\text{SbF}_6)]$	67.2
2	$\text{OPeT}_3$	1	$[\text{BiDipp}_2(\text{SbF}_6)]$	87.3
3	$\text{OPeT}_3$	2	$[\text{BiMe}_2(\text{SbF}_6)]$	51.1
4	$\text{OPeT}_3$	2	$[\text{BiDipp}_2(\text{SbF}_6)]$	52.4
5	$\text{SPMe}_3$	1	$[\text{BiMe}_2(\text{SbF}_6)]$	94.4
6	$\text{SPMe}_3$	1	$[\text{BiDipp}_2(\text{SbF}_6)]$	94.2
7	$\text{SPMe}_3$	2	$[\text{BiMe}_2(\text{SbF}_6)]$	52.6
8	$\text{SPMe}_3$	2	$[\text{BiDipp}_2(\text{SbF}_6)]$	60.6
9	$\text{SePMe}_3$	1	$[\text{BiMe}_2(\text{SbF}_6)]$	76.2
10	$\text{SePMe}_3$	1	$[\text{BiDipp}_2(\text{SbF}_6)]$	81.8
11	$\text{SePMe}_3$	2	$[\text{BiMe}_2(\text{SbF}_6)]$	46.3
12	$\text{SePMe}_3$	2	$[\text{BiDipp}_2(\text{SbF}_6)]$	47.3

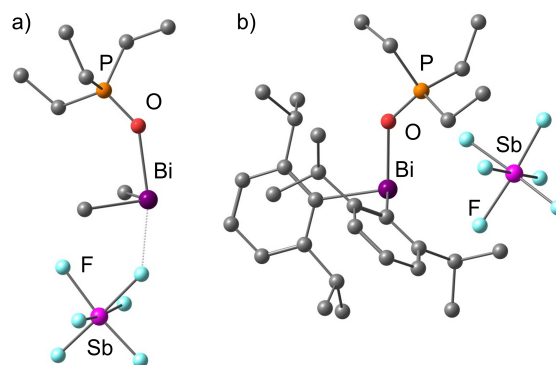


**Figure 6.** Geometry-optimized structures of  $[\text{BiR}_2(\text{OPeT}_3)(\text{SbF}_6)]$ , as obtained from DFT calculations. a)  $\text{R} = \text{Me}$  ( $8_{\text{Me}}$ ); b)  $\text{R} = \text{Dipp}$  ( $8_{\text{Dipp}}$ ).

**Table 2.** Reaction enthalpies and Gibbs energies for adduct formation of the cationic species  $[\text{BiR}_2(\text{Donor})_n(\text{SbF}_6)]$  ( $\text{R} = \text{Me}, \text{Dipp}; n = 0, 1$ ) with donors  $\text{EPR}'_3$  ( $\text{E} = \text{O}, \text{S}, \text{Se}; \text{R}' = \text{Et}, \text{Me}$ ) to give compounds  $[\text{BiR}_2(\text{Donor})_x(\text{SbF}_6)]$  ( $x = 1, 2$ ).

$[\text{BiR}_2(\text{Donor})_n(\text{SbF}_6)]$		$+ (x - n) \text{ equiv. Donor} \rightarrow [\text{BiR}_2(\text{Donor})_x(\text{SbF}_6)]$				
	R	Donor	$n$	$x$	$\Delta H$ [kcal·mol <sup>-1</sup> ]	$\Delta G$ [kcal·mol <sup>-1</sup> ]
1	Me	OPe <sub>3</sub>	0	1	−29.7	−18.3
2	Me	OPe <sub>3</sub>	0	2	−66.5	−42.7
3	Me	OPe <sub>3</sub>	1	2	−36.8	−24.5
4	Me	SPMe <sub>3</sub>	0	1	−19.9	−10.4
5	Me	SPMe <sub>3</sub>	0	2	−51.3	−29.8
6	Me	SPMe <sub>3</sub>	1	2	−31.5	−19.1
7	Me	SePMe <sub>3</sub>	0	1	−21.2	−11.8
8	Me	SePMe <sub>3</sub>	0	2	−56.5	−32.7
9	Me	SePMe <sub>3</sub>	1	2	−35.3	−20.9
10	Dipp	OPe <sub>3</sub>	0	1	−33.1	−19.2
11	Dipp	OPe <sub>3</sub>	0	2	−62.3	−34.5
12	Dipp	OPe <sub>3</sub>	1	2	−29.2	−15.4
13	Dipp	SPMe <sub>3</sub>	0	1	−24.3	−12.9
14	Dipp	SPMe <sub>3</sub>	0	2	−45.9	−19.1
15	Dipp	SPMe <sub>3</sub>	1	2	−21.6	−6.1
16	Dipp	SePMe <sub>3</sub>	0	1	−27.1	−15.1
17	Dipp	SePMe <sub>3</sub>	0	2	−48.3	−21.3
18	Dipp	SePMe <sub>3</sub>	1	2	−21.3	−6.2

featuring bulky Dipp substituents (entries 15, 18). This was ascribed to stronger covalent contributions to Bi–S/SePMe<sub>3</sub> bonding when compared to Bi–OPe<sub>3</sub> bonding. Covalent contributions are more sensitive to changes in interatomic distances, which are relevant in the sterically encumbered complexes  $[\text{BiDipp}_2(\text{EPR}'_3)(\text{SbF}_6)]$  ( $\text{E} = \text{S}$  (**6**<sub>Dipp</sub>),  $\text{Se}$  (**7**<sub>Dipp</sub>)). Significantly larger covalent contributions to Bi–S/SePMe<sub>3</sub> (as compared to Bi–OPe<sub>3</sub>) can be anticipated due to the differences in electronegativity of the donor atoms (O–Se) and were confirmed by distance criteria and atoms-in-molecules analyses (i.e., electron localization function; for details including a discussion of differences in the Laplacian of the electron density, the ratio of potential over kinetic energy density, and the total energy density at the bond critical points see the Supporting Information). These findings are in line with the ligand exchange reactions  $2 [\text{BiDipp}_2(\text{EPR}'_3)](\text{SbF}_6) \rightleftharpoons [\text{BiDipp}_2(\text{SbF}_6)] + [\text{BiDipp}_2(\text{EPR}'_3)_2](\text{SbF}_6)$  becoming increasingly endergonic with increasing softness of the Lewis base ( $\Delta G = +3.8 \text{ kcal} \cdot \text{mol}^{-1}$  ( $\text{E} = \text{O}, \text{R}' = \text{Et}$ ),  $+6.8 \text{ kcal} \cdot \text{mol}^{-1}$  ( $\text{E} = \text{S}, \text{R}' = \text{Me}$ ),  $+9.0 \text{ kcal} \cdot \text{mol}^{-1}$  ( $\text{E} = \text{Se}, \text{R}' = \text{Me}$ )). Thus, the fact that compound  $[\text{BiDipp}_2(\text{OPe}_3)_2](\text{SbF}_6)$  (**8'**<sub>Dipp</sub>) was reproducibly crystallized from solutions containing  $[\text{BiDipp}_2(\text{SbF}_6)]$  and OPe<sub>3</sub> in a 1:1 stoichiometry can be attributed to favorable intermolecular interactions of this species in the solid state.

In order to explore the reactivity of **4**<sub>Dipp</sub> and **I** towards Lewis bases, we turned our attention to isocyanides, which represent important chemical building blocks with relevance for fields such as medicinal chemistry, fragrance, and total synthesis.<sup>[38]</sup> In addition to the rich portfolio of organic compounds that can be derived from isocyanides, their coordination chemistry towards main group metals has been investigated in some detail.<sup>[39]</sup> In contrast, only little is known about the chemistry of isocyanides with heavy main group Lewis acids in general and group 15 species in specific. For instance, the insertion of isocyanides into

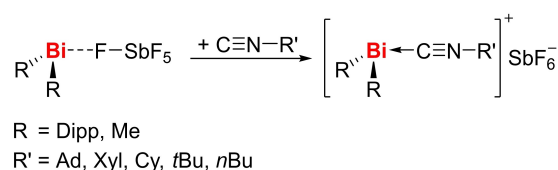
Bi–B and Bi–N bonds has been reported, exploiting the high reactivity of boryl anions<sup>[40]</sup> and ring-strained BiC<sub>2</sub>N cycles.<sup>[10a]</sup> For transition metal stabilized phosphinidenes and arsinidenes, the coordination of CNtBu could be observed, while less bulky isocyanides underwent subsequent insertion reactions.<sup>[41]</sup> Simple Lewis acid/base adducts between bismuth compounds and isocyanides have not been reported to date.

Reaction of **4**<sub>Dipp</sub> and **I** with CNtBu gave **9**<sub>Dipp</sub> and **9**<sub>Me</sub> as isolable Lewis acid/base adducts (Scheme 4). In light of the previously reported importance of steric bulk for the stability of adducts between phosphinidenes and arsinidenes and isocyanides,<sup>[41]</sup> the steric bulk of both, the bismuth cation and the isocyanide CNR', was modified stepwise. The synthesis of **10**<sub>Me</sub> with R' = adamantyl confirmed the accessibility of adducts with sufficient steric bulk, but also compounds **11**<sub>Me</sub>–**13**<sub>Me</sub> with R' = xyl, cyclohexyl, and *n*-butyl could readily be isolated. In all cases that bear aliphatic substituents in the isocyanide, even an excess of this substrate led to the isolation of the mono-adducts, albeit the reversible exchange of isocyanide ligands was apparent from NMR spectroscopic analyses of reactions with a Bi/isocyanide ratio of 1:2. Only in the case of R' = xyl, the mono-adduct **11**<sub>Me</sub> and the bis-adduct **11'**<sub>Me</sub> could be obtained from reactions with a 1:1 and a 1:2 stoichiometry, respectively.

The <sup>1</sup>H and <sup>13</sup>C NMR spectroscopic analyses of the isocyanide adducts **9**–**13** revealed similar trends for all compounds: the signals assigned to the protons of the bismuth-bound isocyanides are slightly shifted towards lower field, while the CNR' carbon atom experiences a strong up-field shift ( $\Delta\delta \approx 70 \text{ ppm}$ , for all monoadducts), when compared to the free compounds.<sup>[42]</sup> The resonances corresponding to the bismuth-bound methyl groups, however, show a considerable upfield shift compared to the starting material **I** and are in most cases close to those of the neutral chlorido species BiMe<sub>2</sub>Cl (**II**; Table 3).

The IR spectroscopic analysis of compounds **9**–**13** revealed a considerable blue-shift of the CN stretching frequency in all cases of mono-adducts ( $\Delta\tilde{\nu} = 80\text{--}108 \text{ cm}^{-1}$ ), indicating ligand to metal  $\sigma$ -donation to be dominant (Table 4).

A closer analysis of all mono-adducts with aliphatic isocyanides reveals that the coordination to the  $[\text{BiMe}_2(\text{SbF}_6)]$  complex fragment results in a blue-shift by 93 to  $108 \text{ cm}^{-1}$  and for CNtBu in specific, in a blue-shift of  $106 \text{ cm}^{-1}$ . In contrast, coordination of this ligand to the  $[\text{BiDipp}_2(\text{SbF}_6)]$  complex fragment shifts the CN stretching frequency by only  $80 \text{ cm}^{-1}$ . This was tentatively ascribed to weak, but significant electron back-donation from the complex fragment  $[\text{BiR}_2(\text{SbF}_6)]$  to the isocyanide, which appears to be more pronounced in the case

**Scheme 4.** Synthesis of isonitrile adducts from  $[\text{BiR}_2(\text{SbF}_6)]$ .

**Table 3.**  $^1\text{H}$  and  $^{13}\text{C}$  NMR chemical shifts of bismuth-bound methyl groups and isocyanide carbon atoms.

Compound	Me (ppm) $^1\text{H}$ NMR	$^{13}\text{C}$ NMR	CNR' (ppm) $^{13}\text{C}$ NMR
$\text{BiMe}_3$ (II)	1.11	−6.82	—
$\text{BiMe}_2\text{Cl}$ (III)	1.80	34.66	—
$[\text{BiMe}_2(\text{SbF}_6)]$ (I)	2.28	64.38	—
$[\text{BiMe}_2(\text{CNtBu})(\text{SbF}_6)]$ ( <b>9</b> <sub>Me</sub> )	1.85	30.01	82.52
$[\text{BiDipp}_2(\text{CNtBu})(\text{SbF}_6)]$ ( <b>9</b> <sub>Dipp</sub> )	0.98 <sup>[b]</sup>	—	— <sup>[a]</sup>
$[\text{BiMe}_2(\text{CNAd})(\text{SbF}_6)]$ ( <b>10</b> <sub>Me</sub> )	1.85	27.25	82.41
$[\text{BiMe}_2(\text{CNXyl})(\text{SbF}_6)]$ ( <b>11</b> <sub>Me</sub> )	2.00	30.82	98.25
$[\text{BiMe}_2(\text{CNXyl})_2(\text{SbF}_6)]$ ( <b>11'</b> <sub>Me</sub> )	1.84	24.40	119.76
$[\text{BiMe}_2(\text{CNCy})(\text{SbF}_6)]$ ( <b>12</b> <sub>Me</sub> )	1.84	31.00	84.23
$[\text{BiMe}_2(n\text{BuNC})(\text{SbF}_6)]$ ( <b>13</b> <sub>Me</sub> )	1.89	22.75	— <sup>[a]</sup>

[a] Signal could not be detected due to broadening. [b] Measured in  $\text{C}_6\text{D}_6$ .**Table 4.** Wavenumbers of the  $\text{C}\equiv\text{N}$  vibration in compounds  $[\text{BiR}_2(\text{C}\equiv\text{NR}')_n(\text{SbF}_6)]$  as determined by FTIR spectroscopy in the solid state.

Compound	Complex ( $\text{C}\equiv\text{N}$ ) [ $\text{cm}^{-1}$ ]	Free isocyanide ( $\text{C}\equiv\text{N}$ ) [ $\text{cm}^{-1}$ ]
$[\text{BiMe}_2(\text{CNtBu})(\text{SbF}_6)]$ ( <b>9</b> <sub>Me</sub> )	2242	2136
$[\text{BiDipp}_2(\text{CNtBu})(\text{SbF}_6)]$ ( <b>9</b> <sub>Dipp</sub> )	2216	2136
$[\text{BiMe}_2(\text{CNAd})(\text{SbF}_6)]$ ( <b>10</b> <sub>Me</sub> )	2229	2121
$[\text{BiMe}_2(\text{CNXyl})(\text{SbF}_6)]$ ( <b>11</b> <sub>Me</sub> )	2203	2120
$[\text{BiMe}_2(\text{CNXyl})_2(\text{SbF}_6)]$ ( <b>11'</b> <sub>Me</sub> )	2175	2120
$[\text{BiMe}_2(\text{CNCy})(\text{SbF}_6)]$ ( <b>12</b> <sub>Me</sub> )	2239	2136
$[\text{BiMe}_2(n\text{BuNC})(\text{SbF}_6)]$ ( <b>13</b> <sub>Me</sub> )	2243	2150

of  $\text{R}=\text{Dipp}$ . This is supported by DFT calculations and molecular orbital analyses of  $[\text{BiR}_2(\text{SbF}_6)]$ , which reveal occupied orbitals relevant for back-donation to be higher in energy for  $\text{R}=\text{Dipp}$  (HOMO−1 to HOMO−5) than for  $\text{R}=\text{Me}$  (HOMO, HOMO−1) by up to 1.2 eV (for details see the Supporting Information). It should be noted that for the Dipp-substituted species, some of these orbitals contain significant contributions by the  $\pi$ -electron cloud of a Dipp ligand that can contribute to back-donation. In the bis-isocyanide adduct **12'**<sub>Me</sub>, an expectedly smaller blue shift of  $\Delta\tilde{\nu}=55\text{ cm}^{-1}$  is observed.

Single-crystal X-ray diffraction of four mono-adducts (**9**<sub>Me</sub>, **9**<sub>Dipp</sub>, **11**<sub>Me</sub>, **12**<sub>Me</sub>) and the bis-adduct (**11'**<sub>Me</sub>) were performed and confirm the connectivity suggested based on spectroscopic data. All compounds show a bisphenoidal coordination geometry around the central bismuth atom, with the isocyanide ligand and the  $[\text{SbF}_6]^-$  counterion (weak  $\text{Bi}\cdots\text{F}$  contact) occupying the axial positions. Selected structural parameters of these compounds are summarized in Table 5.

The bismuth-carbon bond lengths of the  $\text{BiMe}_2/\text{BiDipp}_2$  unit are similar to those in the respective starting material.<sup>[8]</sup> In the mono-adducts, the dative carbon-bismuth bonds are significantly longer, but they are similar to dative  $\text{C}\rightarrow\text{Bi}$  bonds that have been reported for carbene ligands bound to bismuth (2.3545(5)–2.489(6) Å).<sup>[43]</sup> The fourth coordination site at the

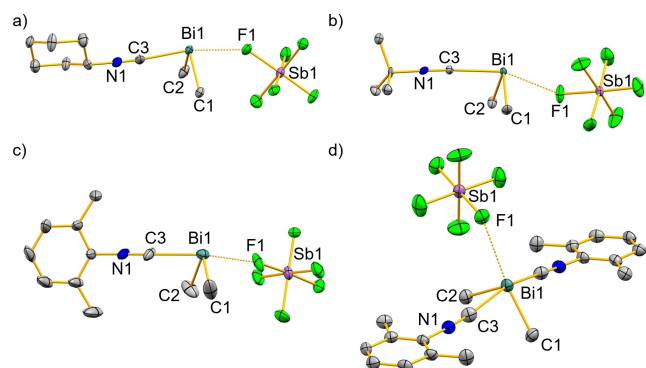
**Table 5.** Selected bond lengths of the isocyanide adducts and parent compounds.

Compound	$\text{Bi}-\text{CH}_3/\text{Dipp}$ [Å]	$\text{Bi}-\text{C}$ [Å]	$\text{Bi}\cdots\text{F}$ [Å]
$[\text{BiMe}_2(\text{SbF}_6)]$ (I)	2.215(5) 2.223(5)	—	2.451(3) 2.452(3)
$[\text{BiDipp}_2(\text{SbF}_6)]$ ( <b>4</b> <sub>Dipp</sub> )	2.257(2) 2.260(2)	—	2.4593(15)
$[\text{BiMe}_2(\text{CNtBu})(\text{SbF}_6)]$ ( <b>9</b> <sub>Me</sub> ) <sup>[a]</sup>	2.2345 2.226	2.369	2.725(5)
$[\text{BiDipp}_2(\text{CNtBu})(\text{SbF}_6)]$ ( <b>9</b> <sub>Dipp</sub> ) <sup>[b]</sup>	2.27(2) 2.28(2)	2.36(2)	3.15(1)
$[\text{BiMe}_2(\text{CNXyl})(\text{SbF}_6)]$ ( <b>11</b> <sub>Me</sub> )	2.230(6) 2.198(7)	2.391(7)	2.540(7)
$[\text{BiMe}_2(\text{CNXyl})_2(\text{SbF}_6)]$ ( <b>11'</b> <sub>Me</sub> )	2.244(5) 2.229(5)	2.568(5) 2.562(5)	3.264(3)
$[\text{BiMe}_2(\text{CNCy})(\text{SbF}_6)]$ ( <b>12</b> <sub>Me</sub> )	2.225(8) 2.220(8)	2.382(9)	2.696(5)

[a] Two molecules in the asymmetric unit. [b] Crystallized as a non-merohedral twin.

bismuth atom is occupied by one fluorine atom of the  $(\text{SbF}_6)^-$  anion, corresponding to a  $\text{Bi}\cdots\text{F}$  interaction based on distance criteria (sum of  $\text{Bi}/\text{F}$  van der Waals radii, 3.54 Å).<sup>[30]</sup> The  $\text{Bi}\cdots\text{F}$  distances reflect the electronic and steric parameters of the  $[\text{BiR}_2(\text{CNR}')^+]$  cations, as they are significantly larger for species with bulky ligands ( $\text{R}=\text{Dipp}$ : 3.15(1) Å) and shorter for compounds with more weakly  $\sigma$ -donating isonitriles ( $\text{R}'=\text{Xyl}$ ; 2.540(7) Å).

The coordination of two isocyanide ligands in **11'**<sub>Me</sub> results in a distorted square pyramidal coordination geometry around bismuth ( $\tau_5=0.19$ ) with one methyl group in the apical position, when weak  $\text{Bi}\cdots\text{F}$  contacts are taken into account (Figure 7). The bismuth-methyl bond lengths are similar to those of the mono-adducts and  $[\text{BiMe}_2(\text{SbF}_6)]$ , that is, the coordination of the isocyanide has very little influence on the length of covalent bismuth-carbon bonds. The dative bismuth-carbon bonds are significantly longer than those in the mono-adduct  $[\text{BiMe}_2(\text{XylNC})(\text{SbF}_6)]$  (**11**<sub>Me</sub>), so the  $\text{RNC}-\text{Bi}$  bond weakening upon introduction of a second isocyanide ligand is clearly reflected by distance criteria in the solid state. The increase in

**Figure 7.** Crystal structures of a) **12**<sub>Me</sub>, b) **9**<sub>Me</sub>, c) **11**<sub>Me</sub>, and d) **11'**<sub>Me</sub>. Displacement ellipsoids are drawn at the 50% probability level, H atoms are omitted for clarity. Selected bond lengths are shown in Table 5.

coordination number (as compared to the mono-isocyanide-adducts) results in an elongation of the bismuth...fluorine distance (3.264(3) Å).

The straightforward Lewis pair formation presented here not only gives access to bismuth-bound isocyanides, but could be extended to generate isolable phosphane and nitrile adducts of **4**<sub>Dipp</sub> and **I** (see the Supporting Information). As isocyanides are isolable with carbon monoxide, adduct formation was also attempted. However, first reactions between **4**<sub>Dipp</sub> or **I** and CO have not led to isolable products so far.

## Conclusion

In conclusion, we have synthesized the donor-free bismuth cation [BiR<sub>2</sub>(SbF<sub>6</sub>)] with bulky aryl ligands (R=Dipp=2,6-*i*Pr-C<sub>6</sub>H<sub>3</sub>). The Lewis acidity of this compound (R=Dipp) and its methyl analogue (R=Me) have been investigated, revealing a remarkable impact of steric bulk: according to Gutmann-Beckett analyses combined with DFT calculations, the steric profile of [BiDipp<sub>2</sub>(SbF<sub>6</sub>)] boosts its Lewis acidity compared to [BiMe<sub>2</sub>(SbF<sub>6</sub>)] by protecting one lobe of the vacant p-orbital in the cationic complex fragment [BiDipp<sub>2</sub>]<sup>+</sup>, a phenomenon that is most pronounced towards the hard donor OPET<sub>3</sub>. The weakly coordinating anion (PF<sub>6</sub>)<sup>−</sup> is shown to be unsuitable for the stabilization of bismuth cations [BiR<sub>2</sub>]<sup>+</sup> due to stepwise fluoride ion abstraction, yielding the unprecedented structural motif [R<sub>2</sub>Bi–F–BiR<sub>2</sub>]<sup>+</sup> with a remarkable flexibility of the Bi–F–Bi angle. Reactions of [BiR<sub>2</sub>(SbF<sub>6</sub>)] with Lewis bases resulted in facile Lewis pair formation. This gave access to the first set of compounds featuring isocyanide ligands CNR' in the coordination sphere of softly Lewis acidic bismuth cations, thus offering prospects for functionalization in subsequent reactions. It is anticipated that these results will facilitate and stimulate the design of Lewis acids and the application of cationic bismuth species as reagents and catalysts in chemical synthesis.

## Experimental Section

If not stated otherwise, all experiments were conducted under dry argon using Schlenk and glovebox techniques. Solvents were degassed and purified according to standard laboratory procedures. NMR spectra were recorded on Bruker Avance spectrometers operating at 400 or 500 MHz with respect to <sup>1</sup>H. <sup>1</sup>H and <sup>13</sup>C NMR chemical shifts are reported relative to SiMe<sub>4</sub> using the residual signal of the deuterated solvent as a secondary standard. <sup>19</sup>F and <sup>31</sup>P NMR chemical shifts are reported relative to CFCl<sub>3</sub> and 85% aqueous H<sub>3</sub>PO<sub>4</sub>, respectively, as external standards. Infrared spectra were recorded on a Bruker Alpha P spectrometer. Elemental analyses were performed on a vario MICRO cube. Single-crystals suitable for X-ray diffraction were coated with polyisobutylene or perfluorinated polyether oil in a glovebox, transferred to a nylon loop and then transferred to the goniometer of a diffractometer equipped with either a molybdenum (λ = 0.71073 Å) or copper (λ = 1.54184 Å) X-ray tube. The structure was solved using intrinsic phasing methods and expanded using Fourier techniques.<sup>[44]</sup> All non-hydrogen atoms were refined anisotropically. Hydrogen atoms were included in structure factors calculations. All hydrogen atoms were assigned to idealized geometric positions.

Deposition Numbers 2232014 (for **4**-tol<sub>Dipp</sub>), 2232015 (for **11'**<sub>Me</sub>), 2232016 (for **5**<sub>Dipp</sub>), 2232017 (for **3**<sub>Dipp</sub>), 2232018 (for **11**<sub>Me</sub>), 2232019 (for **8'**<sub>Dipp</sub>), 2232020 (for **7**<sub>Dipp</sub>), 2232021 (for **9**<sub>Me</sub>), 2232022 (for **14**<sub>Me</sub>), 2232023 (for **6**<sub>Dipp</sub>), 2232024 (for **9**<sub>Dipp</sub>), 2232025 (for **12**<sub>Me</sub>), 2232026 (for **4**<sub>Dipp</sub>), 2232027 (for **2**<sub>Dipp</sub>), and 2232028 (for **16**<sub>Dipp</sub>) contain the supplementary crystallographic data for this paper. These data are provided free of charge by the joint Cambridge Crystallographic Data Centre and Fachinformationszentrum Karlsruhe Access Structures service.

**General procedure to determine the acceptor numbers:** [BiMe<sub>2</sub>(SbF<sub>6</sub>)] (30 mg, 0.06 mmol, 1 equiv.) was dissolved in dichloromethane (5 mL). One or two equivalents, respectively (see main text), of the (modified) Gutmann-Beckett reagents (OPET<sub>3</sub>, SPMe<sub>3</sub>, SePMe<sub>3</sub>) was added as well as a capillary filled with 85% aqueous H<sub>3</sub>PO<sub>4</sub>. After addition the yellow solution quickly turned colorless. Without further purification <sup>1</sup>H (to ensure the formation of a monoadduct) and <sup>31</sup>P NMR spectra were measured. The acceptor numbers were calculated using the <sup>31</sup>P NMR chemical shifts and the following formulas: OPET<sub>3</sub>: AN = 2.21 (δ<sub>p</sub> −41.0); SPMe<sub>3</sub>: AN = 6.41 (δ<sub>p</sub> −29.2); SePMe<sub>3</sub>: AN = 5.71 (δ<sub>p</sub> −7.8).

**Attempted preparation of [BiDipp<sub>2</sub>(PF<sub>6</sub>)]** **1**<sub>Dipp</sub>: Dipp<sub>2</sub>BiBr (200 mg, 0.33 mmol) was dissolved in 6 mL toluene and solid Ag[PF<sub>6</sub>] (83 mg, 0.33 mmol) was added in small batches under constant stirring. After the removal of precipitates by filtration and of volatiles under reduced pressure, a red solid was obtained. The solid supposedly consists mainly of **1**<sub>Dipp</sub>. However, upon storage under inert atmosphere or attempted purification decomposition of **1**<sub>Dipp</sub> to unidentified products, **2**<sub>Dipp</sub> and Dipp<sub>2</sub>BiF was observed. Yield: 80% (278 mg, 0.26 mmol). <sup>1</sup>H NMR (300 MHz, [D<sub>8</sub>]tol): δ = 1.06 (d, <sup>3</sup>J<sub>H-H</sub> = 6.4 Hz, 24H, *o*-CCH(CH<sub>3</sub>)<sub>2</sub>), 2.71 (sept, <sup>3</sup>J<sub>H-H</sub> = 6.4 Hz, 4H, *o*-CCH(CH<sub>3</sub>)<sub>2</sub>), 7.42 (t, <sup>3</sup>J<sub>H-H</sub> = 7.6 Hz, 2H, *p*-CH), 7.88 ppm (d, <sup>3</sup>J<sub>H-H</sub> = 7.6 Hz, 4H, *m*-CH); <sup>13</sup>C{<sup>1</sup>H} NMR (125 MHz, [D<sub>8</sub>]tol): δ = 24.7 (s, *o*-CCH(CH<sub>3</sub>)<sub>2</sub>), 38.1 (s, *o*-CCH(CH<sub>3</sub>)<sub>2</sub>), 130.0 (s, *o*-CCH(CH<sub>3</sub>)<sub>2</sub>), 132.7 (s, *p*-CH), 157.6 ppm (s, *m*-CH), (Bi-C, not found); <sup>31</sup>P{<sup>1</sup>H} NMR (122 MHz, [D<sub>8</sub>]tol): δ = −139.8 (sept, <sup>1</sup>J<sub>P-F</sub> = 730.1 Hz, PF<sub>6</sub>), <sup>19</sup>F NMR (282 MHz [D<sub>8</sub>]tol): δ = −69.9 (d, <sup>1</sup>J<sub>P-F</sub> = 728.6 Hz, PF<sub>6</sub>).

**[BiDipp<sub>2</sub>(OPET<sub>3</sub>)<sub>2</sub>(PF<sub>6</sub>)]** (**3**<sub>Dipp</sub>): BiDipp<sub>2</sub>Br (250 mg, 0.41 mmol) and triethylphosphaneoxide (88 mg, 0.82 mmol) were dissolved in 8 mL THF, and AgPF<sub>6</sub> (104 mg, 0.41 mmol) in THF (6 mL) was added dropwise at room temperature. After stirring for 90 min, precipitates were filtered off and all volatiles were removed under reduced pressure. The remaining colorless solid was recrystallized from a mixture of toluene and pentane, and **3**<sub>Dipp</sub> was obtained in the form of colorless crystals. Yield: 71% (241 mg, 0.29 mmol). <sup>1</sup>H NMR (300 MHz, C<sub>6</sub>D<sub>6</sub>): δ = 0.84 (dq, <sup>3</sup>J<sub>H-H</sub> = 7.7 Hz, <sup>3</sup>J<sub>P-H</sub> = 11.7 Hz, 18H, PCH<sub>2</sub>CH<sub>3</sub>), 1.09 (d, <sup>3</sup>J<sub>H-H</sub> = 6.4 Hz, 24H, *o*-CCH(CH<sub>3</sub>)<sub>2</sub>), 1.58 (dq, <sup>3</sup>J<sub>H-H</sub> = 7.7 Hz, <sup>2</sup>J<sub>P-H</sub> = 11.7 Hz, 12H, PCH<sub>2</sub>CH<sub>3</sub>), 3.14 (sept, <sup>3</sup>J<sub>H-H</sub> = 6.4 Hz, 4H, *o*-CCH(CH<sub>3</sub>)<sub>2</sub>), 7.33 (t, <sup>3</sup>J<sub>H-H</sub> = 7.6 Hz, 2H, *p*-CH), 7.60 ppm (d, <sup>3</sup>J<sub>H-H</sub> = 7.6 Hz, 4H, *m*-CH); <sup>13</sup>C{<sup>1</sup>H} NMR (75 MHz, C<sub>6</sub>D<sub>6</sub>): δ = 5.6 (d, <sup>2</sup>J<sub>P-C</sub> = 5.1 Hz, PCH<sub>2</sub>CH<sub>3</sub>), 19.0 (d, <sup>1</sup>J<sub>P-C</sub> = 65.6 Hz, PCH<sub>2</sub>CH<sub>3</sub>), 25.0 (s, *o*-CCH(CH<sub>3</sub>)<sub>2</sub>), 37.5 (s, 4 C, *o*-CCH(CH<sub>3</sub>)<sub>2</sub>), 129.4 (s, *o*-CCH(CH<sub>3</sub>)<sub>2</sub>), 129.9 (s, *p*-CH), 157.2 (s, *m*-CH), 206.0 ppm (s, Bi-C); <sup>31</sup>P{<sup>1</sup>H} NMR (122 MHz, C<sub>6</sub>D<sub>6</sub>): δ = −142.4 (sept, <sup>1</sup>J<sub>P-F</sub> = 712.1 Hz, PF<sub>6</sub>), 66.3 (s, OPET<sub>3</sub>); Elemental analysis calcd (%) for [C<sub>36</sub>H<sub>64</sub>BiF<sub>6</sub>O<sub>3</sub>P<sub>3</sub>] (944.80 g/mol): C 45.77, H 6.83; found: C 45.84, H 6.90; IR (cm<sup>−1</sup>)  $\bar{\nu}$  = 3038.63 (w), 2965.56 (w), 2946.82 (w), 2923.95 (w), 2882.98 (w), 2865.05 (w), 1569.02 (w), 1457.91 (m), 1446.08 (w), 1409.99 (w), 1381.18 (w), 1359.59 (w), 1270.45 (w), 1237.22 (w), 1175.07 (w), 1146.71 (w), 1089.96 (w), 1069.81 (s), 1044.60 (s), 1033.49 (s), 984.84 (m), 921.66 (s), 872.89 (w), 794.35 (w), 780.44 (w), 725.66 (w), 555.56 (s), 447.72 (m); HR-MS: Cl(+) *m/z* 531.2461 [Dipp<sub>2</sub>Bi]<sup>+</sup>; calcd 531.2464; *m/z* 135.0966 [Et<sub>3</sub>PO]<sup>+</sup>; calcd 135.0939.

**[BiDipp<sub>2</sub>][SbF<sub>6</sub>]** (**4**<sub>Dipp</sub>): BiDipp<sub>2</sub>Br (400 mg, 0.64 mmol) was dissolved in toluene (50 mL) and solid Ag[SbF<sub>6</sub>] (220 mg, 0.64 mmol) was

added in small batches under constant stirring, whereupon the orange solution turned dark red. After stirring for 90 min, the solution was filtered and concentrated under reduced pressure. Storage at  $-32^{\circ}\text{C}$  for two days yielded dark red crystals of **4-tol**<sub>Dipp</sub>. Yield: 59% (330 mg, 0.38 mmol). Crystalline **4**<sub>Dipp</sub> was obtained by recrystallization from  $\alpha,\alpha,\alpha$ -trifluorotoluene.  $^1\text{H}$  NMR (500 MHz,  $\text{C}_6\text{D}_6$ ):  $\delta$  = 1.06 (d,  $^3J_{\text{H-H}}$  = 6.4 Hz, 24H, *o*-CCH( $\text{CH}_3$ )<sub>2</sub>), 2.53 (sept,  $^3J_{\text{H-H}}$  = 6.4 Hz, 4H, *o*-CCH( $\text{CH}_3$ )<sub>2</sub>), 7.51 (t,  $^3J_{\text{H-H}}$  = 7.6 Hz, 2H, *p*-CH), 8.08 ppm (d,  $^3J_{\text{H-H}}$  = 7.6 Hz, 4H, *m*-CH);  $^{13}\text{C}\{^1\text{H}\}$  NMR (125 MHz,  $\text{C}_6\text{D}_6$ ):  $\delta$  = 23.9 (s, *o*-CCH( $\text{CH}_3$ )<sub>2</sub>), 38.8 (s, *o*-CCH( $\text{CH}_3$ )<sub>2</sub>), 130.3 (s, *o*-CCH( $\text{CH}_3$ )<sub>2</sub>), 134.3 (s, *p*-CH), 158.0 (s, *m*-CH), 238.1 ppm (s, Bi-C);  $^{19}\text{F}$  NMR (470 MHz):  $\delta$  =  $-120.8$  ppm (brs,  $\text{SbF}_6$ );  $^1\text{H}$  NMR (500 MHz,  $\text{CD}_2\text{Cl}_2$ ):  $\delta$  = 1.21 (d,  $^3J_{\text{H-H}}$  = 6.4 Hz, 24H, *o*-CCH( $\text{CH}_3$ )<sub>2</sub>); 2.65 (sept,  $^3J_{\text{H-H}}$  = 6.4 Hz, 4H, *o*-CCH( $\text{CH}_3$ )<sub>2</sub>), 8.00 (t,  $^3J_{\text{H-H}}$  = 7.7 Hz, 2H, *p*-CH), 8.61 ppm (d,  $^3J_{\text{H-H}}$  = 7.7 Hz, 4H, *m*-CH);  $^{13}\text{C}\{^1\text{H}\}$  NMR (125 MHz,  $\text{CD}_2\text{Cl}_2$ ):  $\delta$  = 24.0 (s, *o*-CCH( $\text{CH}_3$ )<sub>2</sub>); 39.6 (s, *o*-CCH( $\text{CH}_3$ )<sub>2</sub>), 131.0 (s, *o*-CCH( $\text{CH}_3$ )<sub>2</sub>), 135.3 (s, *p*-CH), 158.5 (s, *m*-CH), 237.6 ppm (s, Bi-C);  $^{19}\text{F}$  NMR (470 MHz):  $\delta$  =  $-123.0$  ppm (brs,  $\text{SbF}_6$ ); elemental analysis calcd (%) for  $\text{C}_{24}\text{H}_{34}\text{BiF}_6\text{Sb}$  (767.27 g/mol): C 37.57, H 4.47; found: C 37.28, H 4.50; IR ( $\text{cm}^{-1}$ ): 3046 (w), 2960 (m), 2927 (w), 2867 (w), 1570 (w), 1459 (m), 1447 (m), 1415 (w), 1384 (w), 1364 (w), 1343 (w), 1241 (w), 1177 (w), 1147 (w), 1046 (w), 1001 (w), 931 (s), 797 (s), 726 (s), 623 (s), 490 (w).

**[(BiDipp)<sub>2</sub>F(SbF<sub>6</sub>)] (5<sub>Dipp</sub>):** Compound **4-tol** (40 mg, 0.05 mmol) was suspended in toluene (2 mL), and BiDipp<sub>2</sub>F (26 mg, 0.05 mmol) in toluene (2 mL) was added, leading to the precipitation of an orange crystalline solid. After 2 h of stirring and complete consumption of the dark red **4-tol**, liquids were removed by decanting with a syringe. The remaining solid was washed twice with pentane (5 mL) and dried under reduced pressure. Yield: 72% (44 mg, 0.03 mmol).  $^1\text{H}$  NMR (500 MHz,  $\text{CD}_2\text{Cl}_2$ ):  $\delta$  = 1.08 ppm (d,  $^3J_{\text{H-H}}$  = 6.4 Hz, *o*-CCH( $\text{CH}_3$ )<sub>2</sub>), 2.72 (t,  $^3J_{\text{H-H}}$  = 6.6 Hz, 4H, *o*-CCH( $\text{CH}_3$ )<sub>2</sub>), 7.73 (t,  $^3J_{\text{H-H}}$  = 7.6 Hz, 2H, *p*-CH), 8.10 ppm (d,  $^3J_{\text{H-H}}$  = 7.6 Hz, 4H, *m*-CH);  $^{13}\text{C}\{^1\text{H}\}$  NMR (125 MHz,  $\text{CD}_2\text{Cl}_2$ ):  $\delta$  = 24.4 (s, *o*-CCH( $\text{CH}_3$ )<sub>2</sub>), 38.0 (s, *o*-CCH( $\text{CH}_3$ )<sub>2</sub>), 130.6 (s, *o*-CCH( $\text{CH}_3$ )<sub>2</sub>), 132.6 (s, *p*-CH), 157.2 (s, *m*-CH), 215.8 ppm (Bi-C, found by HMBC);  $^{19}\text{F}$  NMR (282 MHz,  $\text{CD}_2\text{Cl}_2$ ):  $\delta$  =  $-122.3$  (brs,  $\text{SbF}_6$ ),  $-216.1$  ppm (brs, Bi-F); elemental analysis calcd (%) for  $[\text{C}_{48}\text{H}_{68}\text{Bi}_2\text{F}_7\text{Sb}]$  (1317.77 g/mol): C 43.75; H 5.20; found: C 43.94; H 5.16; IR ( $\text{cm}^{-1}$ ): 3046 (w), 2960 (m), 2927 (w), 2867 (w), 1570 (w), 1459 (m), 1447 (m), 1415 (w), 1384 (w), 1364 (w), 1343 (w), 1241 (w), 1177 (w), 1147 (w), 1046 (w), 1001 (w), 931 (w), 797 (m), 726 (s), 623 (s), 490 (w).

**General procedure for the preparation of [BiDipp<sub>2</sub>(EPMe<sub>3</sub>)](SbF<sub>6</sub>):** Compound **4-tol** (50 mg, 0.06 mmol) and EPMe<sub>3</sub> (E = S, Se, 0.06 mmol) were dissolved in DCM (3 mL) at room temperature. The yellow solution was layered with *n*-pentane and stored at  $-32^{\circ}\text{C}$ . After two days, yellow crystals of the products **6**<sub>Dipp</sub> and **7**<sub>Dipp</sub> were obtained.

**[BiDipp<sub>2</sub>(SPMe<sub>3</sub>)](SbF<sub>6</sub>) (6<sub>Dipp</sub>):** Yield: 92% (47 mg, 0.05 mmol).  $^1\text{H}$  NMR (500 MHz,  $\text{CD}_2\text{Cl}_2$ ):  $\delta$  = 1.11 (d,  $^3J_{\text{H-H}}$  = 6.6 Hz, 24H, *o*-CCH( $\text{CH}_3$ )<sub>2</sub>), 2.15 (d,  $^2J_{\text{P-H}}$  = 13.3 Hz, 9H, SP( $\text{CH}_3$ )<sub>3</sub>), 2.92 (sept,  $^3J_{\text{H-H}}$  = 6.6 Hz, 4H, *o*-CCH( $\text{CH}_3$ )<sub>2</sub>), 7.51 (t,  $^3J_{\text{H-H}}$  = 7.6 Hz, 2H, *p*-CH), 7.69 ppm (d,  $^3J_{\text{H-H}}$  = 7.6 Hz, 4H, *m*-CH);  $^{13}\text{C}\{^1\text{H}\}$  NMR (125 MHz,  $\text{CD}_2\text{Cl}_2$ ):  $\delta$  = 19.2 (d,  $^1J_{\text{P-C}}$  = 54.2 Hz, SP( $\text{CH}_3$ )<sub>3</sub>), 24.7 (s, *o*-CCH( $\text{CH}_3$ )<sub>2</sub>), 40.6 (s, *o*-CCH( $\text{CH}_3$ )<sub>2</sub>), 129.4 (s, *o*-CCH( $\text{CH}_3$ )<sub>2</sub>), 130.4 (s, *p*-CH), 156.3 (s, *m*-CH), 183.1 ppm (s, Bi-C);  $^{31}\text{P}$  NMR (202 MHz,  $\text{CD}_2\text{Cl}_2$ ):  $\delta$  = 43.9 ppm (s, SPMe<sub>3</sub>); elemental analysis calcd (%) for  $[\text{C}_{27}\text{H}_{43}\text{BiF}_6\text{P}_2\text{S}_2\text{Sb}]$  (875.40 g/mol): C 37.05; H 4.95; S 3.66; found: C 36.67; H 5.13; S 3.54; IR ( $\text{cm}^{-1}$ ): 3051 (w), 3008 (m), 2960 (w), 2922 (w), 2868 (w), 1569 (w), 1462 (w), 1442 (w), 1410 (w), 1384 (w), 1363 (w), 1342 (w), 1317 (w), 1300 (w), 1235 (w), 1181 (w), 1148 (w), 1048 (w), 1000 (w), 948 (s), 858 (w), 807 (m), 758 (w), 733 (w), 691 (w), 653 (s), 521 (w).

**[BiDipp<sub>2</sub>(SePMe<sub>3</sub>)](SbF<sub>6</sub>) (7<sub>Dipp</sub>):** Yield: 59% (32 mg, 0.03 mmol).  $^1\text{H}$  NMR (500 MHz,  $\text{CD}_2\text{Cl}_2$ ):  $\delta$  = 1.10 (d,  $^3J_{\text{H-H}}$  = 6.6 Hz, 24H, *o*-

CCH( $\text{CH}_3$ )<sub>2</sub>), 2.32 (d,  $^2J_{\text{P-H}}$  = 13.5 Hz, 9H, SeP( $\text{CH}_3$ )<sub>3</sub>), 2.95 (sept,  $^3J_{\text{H-H}}$  = 6.6 Hz, 4H, *o*-CCH( $\text{CH}_3$ )<sub>2</sub>), 7.48 (t,  $^3J_{\text{H-H}}$  = 7.6 Hz, 2H, *p*-CH), 7.65 ppm (d,  $^3J_{\text{H-H}}$  = 7.6 Hz, 4H, *m*-CH);  $^{13}\text{C}\{^1\text{H}\}$  NMR (125 MHz,  $\text{CD}_2\text{Cl}_2$ ):  $\delta$  = 18.8 (d,  $^1J_{\text{P-C}}$  = 47.9 Hz, SeP( $\text{CH}_3$ )<sub>3</sub>), 24.8 (s, *o*-CCH( $\text{CH}_3$ )<sub>2</sub>), 41.4 (s, *o*-CCH( $\text{CH}_3$ )<sub>2</sub>), 128.9 (s, *o*-CCH( $\text{CH}_3$ )<sub>2</sub>), 130.3 (s, *p*-CH), 156.2 (s, *m*-CH), 178.2 ppm (s, Bi-C);  $^{31}\text{P}$  NMR (202 MHz,  $\text{CD}_2\text{Cl}_2$ ):  $\delta$  = 22.13 ppm (s,  $^1J_{\text{P-Se}}$  = 485.1 Hz, SePMe<sub>3</sub>); elemental analysis calcd (%) for  $[\text{C}_{27}\text{H}_{43}\text{BiF}_6\text{P}_2\text{Se}_2\text{Sb}]$  (922.29 g/mol): C 35.16; H 4.70; found: C 35.17; H 4.79; IR ( $\text{cm}^{-1}$ ): 2960 (m), 2920 (w), 2885 (w), 2867 (w), 1583 (w), 1569 (w), 1462 (w), 1441 (w), 1410 (w), 1383 (w), 1363 (w), 1297 (w), 1260 (w), 1235 (m), 1180 (w), 1150 (w), 1100 (w), 1048 (w), 1019 (w), 1000 (w), 947 (s), 857 (w), 806 (s), 758 (w), 733 (w), 652 (s), 641 (s), 503 (w), 494 (w).

**[BiDipp<sub>2</sub>(OPET<sub>3</sub>)<sub>2</sub>(SbF<sub>6</sub>)] (8<sub>Dipp</sub>):** Dipp<sub>2</sub>BiBr (162 mg, 0.26 mmol) and triethylphosphaneoxide (70 mg, 0.52 mmol) were dissolved in THF (8 mL). A solution of AgSbF<sub>6</sub> (90 mg, 0.26 mmol) in THF (6 mL) was added dropwise at room temperature. After stirring for 90 min, volatiles were removed. Toluene (20 mL) was added, and the suspension was filtered. The filtrate was concentrated and stored at  $-32^{\circ}\text{C}$  to give colorless crystals after 2 d, which were isolated by decantation and dried in vacuo. Yield 71% (196 mg, 0.19 mmol).  $^1\text{H}$  NMR (300 MHz,  $\text{C}_6\text{D}_6$ ):  $\delta$  = 0.80 (dt,  $^3J_{\text{H-H}}$  = 7.7 Hz,  $^3J_{\text{P-H}}$  = 17.2 Hz, 18H, PCH<sub>2</sub>CH<sub>3</sub>), 1.08 (d,  $^3J_{\text{H-H}}$  = 6.4 Hz, 24H, *o*-CCH( $\text{CH}_3$ )<sub>2</sub>), 1.49 (dq,  $^3J_{\text{H-H}}$  = 7.6 Hz,  $^2J_{\text{P-H}}$  = 11.7 Hz, 12H, PCH<sub>2</sub>CH<sub>3</sub>), 3.11 (sept,  $^3J_{\text{H-H}}$  = 6.5 Hz, 4H, *o*-CCH( $\text{CH}_3$ )<sub>2</sub>), 7.33 (t,  $^3J_{\text{H-H}}$  = 7.6 Hz, 2H, *m*-CH), 7.59 ppm (d,  $^3J_{\text{H-H}}$  = 7.6 Hz, 4H, *p*-CH);  $^{13}\text{C}\{^1\text{H}\}$  NMR (125 MHz,  $\text{C}_6\text{D}_6$ ):  $\delta$  = 5.6 (d,  $^3J_{\text{P-C}}$  = 4.0 Hz, PCH<sub>2</sub>CH<sub>3</sub>), 19.0 (d,  $^2J_{\text{P-C}}$  = 65.6 Hz, PCH<sub>2</sub>CH<sub>3</sub>), 25.0 (brs, *o*-CCH( $\text{CH}_3$ )<sub>2</sub>), 37.6 (s, *o*-CCH( $\text{CH}_3$ )<sub>2</sub>), 129.5 (s, *o*-CH), 129.9 (s, *p*-CH), 157.0 (s, *m*-CH), 205.6 (s, Bi-C), ppm;  $^{31}\text{P}\{^1\text{H}\}$  NMR (101 MHz,  $\text{C}_6\text{D}_6$ ):  $\delta$  = 65.3 ppm (s, 1P, OPET<sub>3</sub>);  $^1\text{H}$  NMR (500 MHz,  $\text{CD}_2\text{Cl}_2$ ):  $\delta$  = 1.09 (d,  $^3J_{\text{H-H}}$  = 6.4 Hz, 24H, *o*-CCH( $\text{CH}_3$ )<sub>2</sub>), 1.11 (dt,  $^3J_{\text{H-H}}$  = 7.7 Hz,  $^3J_{\text{P-H}}$  = 17.1 Hz, 18H, PCH<sub>2</sub>CH<sub>3</sub>), 1.80 (dq,  $^3J_{\text{H-H}}$  = 7.7 Hz,  $^2J_{\text{P-H}}$  = 11.6 Hz, 12H, PCH<sub>2</sub>CH<sub>3</sub>), 2.96 (sept,  $^3J_{\text{H-H}}$  = 6.4 Hz, 4H, *o*-CCH( $\text{CH}_3$ )<sub>2</sub>), 7.55 (t,  $^3J_{\text{H-H}}$  = 7.6 Hz, 2H, *p*-CH), 7.79 ppm (d,  $^3J_{\text{H-H}}$  = 7.6 Hz, 4H, *m*-CH);  $^{13}\text{C}\{^1\text{H}\}$  NMR (125 MHz,  $\text{CD}_2\text{Cl}_2$ ):  $\delta$  = 5.7 (d,  $^2J_{\text{P-C}}$  = 4.8 Hz, PCH<sub>2</sub>CH<sub>3</sub>), 19.5 (d,  $^1J_{\text{P-C}}$  = 65.6 Hz, PCH<sub>2</sub>CH<sub>3</sub>), 24.6 (s, *o*-CCH( $\text{CH}_3$ )<sub>2</sub>), 37.4 (s, *o*-CCH( $\text{CH}_3$ )<sub>2</sub>), 130.1 (s, *o*-CH), 130.5 (s, *p*-CH), 156.6 (s, *m*-CH), 201.5 ppm (s, Bi-C);  $^{31}\text{P}\{^1\text{H}\}$  NMR (202 MHz,  $\text{CD}_2\text{Cl}_2$ ):  $\delta$  = 65.2 ppm (s, 1P, OPET<sub>3</sub>); elemental analysis calcd (%) for  $[\text{C}_{36}\text{H}_{64}\text{BiF}_6\text{O}_2\text{P}_2\text{Sb}]$  (1035.58 g/mol): C 41.75; H 6.23; found: C 41.77; H 6.44; IR ( $\text{cm}^{-1}$ ): 3039 (w), 2964 (m), 2947 (w), 2924 (w), 2883 (w), 2865 (w), 1569 (w), 1458 (m), 1448 (w), 1410 (w), 1382 (w), 1360 (w), 1270 (w), 1237 (w), 1093 (m), 1070 (m), 1045 (m), 1032 (m), 985 (m), 928 (w), 796 (w), 778 (w), 768 (w), 726 (m), 650 (s), 446 (m), 406 (w).

**[BiDipp<sub>2</sub>(Cn<sup>t</sup>Bu)(SbF<sub>6</sub>)] (9<sub>Dipp</sub>):** Compound **4-tol**<sub>Dipp</sub> (30 mg, 35  $\mu\text{mol}$ ) is dissolved in 2 mL of toluene and Cn<sup>t</sup>Bu (2.9 mg, 35  $\mu\text{mol}$ ) in 0.2 mL of toluene is slowly added. Upon addition, the solution turns orange and some precipitating solids are removed by decanting the toluene solution. After evaporation of volatiles, **9**<sub>Dipp</sub> is obtained as an off-white solid. Yield: 57% (17 mg, 20  $\mu\text{mol}$ ).  $^1\text{H}$  NMR (500 MHz,  $\text{C}_6\text{D}_6$ ):  $\delta$  = 0.98 (d,  $^3J_{\text{H-H}}$  = 6.6 Hz, 24H, *o*-CCH( $\text{CH}_3$ )<sub>2</sub>), 0.98 (s, 9H, C( $\text{CH}_3$ )<sub>3</sub>), 2.70 (sept,  $^3J_{\text{H-H}}$  = 6.6 Hz, 4H, *o*-CCH( $\text{CH}_3$ )<sub>2</sub>), 7.22 (t,  $^3J_{\text{H-H}}$  = 7.6 Hz, 2H, *p*-CH), 7.46 (d,  $^3J_{\text{H-H}}$  = 7.6 Hz, ppm 4H, *m*-CH);  $^{13}\text{C}\{^1\text{H}\}$  NMR (125 MHz,  $\text{C}_6\text{D}_6$ ):  $\delta$  = 24.3 (s, *o*-CCH( $\text{CH}_3$ )<sub>2</sub>), 28.9 (s, C( $\text{CH}_3$ )<sub>3</sub>), 60.8 (s, C( $\text{CH}_3$ )<sub>3</sub>, found by HMBC), 41.0 (s, *o*-CCH( $\text{CH}_3$ )<sub>2</sub>), 124.2 (s, *o*-CCH( $\text{CH}_3$ )<sub>2</sub>), 130.4 (s, *p*-CH), 156.3 (s, *m*-CH), 183.1 ppm (s, Bi-C); elemental analysis calcd (%) for  $[\text{C}_{29}\text{H}_{43}\text{BiF}_6\text{N}_2\text{Sb}]$  (850.40 g/mol): C 40.96; H 5.10; N 1.65; found: C 39.77; H 4.80; N 2.36; IR ( $\text{cm}^{-1}$ ): 3054 (w), 3043 (m), 2966 (w), 2929 (w), 2905 (w), 2866 (w), 2216 (w), 1570 (w), 1460 (w), 1446 (w), 1412 (w), 1376 (w), 1364 (w), 1342 (w), 1236 (m), 1183 (m), 1147 (w), 1046 (w), 1001 (w), 984 (w), 930 (w), 826 (w), 806 (w), 797 (w), 729 (w), 685 (w), 651 (s), 563 (w), 526 (w), 503 (w), 419 (w).

**General procedure for the synthesis of [BiMe<sub>2</sub>(SbF<sub>6</sub>)] adducts:** [BiMe<sub>2</sub>(SbF<sub>6</sub>)] was dissolved in benzene (typically 8 mL). A solution

of the required isocyanide or phosphane in benzene (typically 4 mL) was added. The end of the reaction was determined by either a change in color or formation of a precipitate. Afterwards all volatiles were removed in vacuo and the remaining solid washed with pentane. Drying at  $10^{-3}$  mbar yields the respective product. If there were any deviations from this procedure, this is noted below for the individual compounds.

**[BiMe<sub>2</sub>(Cn<sup>t</sup>Bu)(SbF<sub>6</sub>)] (9<sub>Me</sub>):** [BiMe<sub>2</sub>(SbF<sub>6</sub>): 50 mg, 0.11 mmol, 1 equiv.; *tert*-butylisocyanide: 9 mg, 12  $\mu$ L, 0.11 mmol, 1 equiv. The synthesis was conducted in toluene, during the reaction the solution turned colorless. The crude product was recrystallized from dichloromethane/pentane. Yield: 45 mg (0.08 mmol, 72%) of an orange solid. <sup>1</sup>H NMR (500 MHz, CD<sub>2</sub>Cl<sub>2</sub>):  $\delta$  = 1.58 (s, 9H, CNC(CH<sub>3</sub>)<sub>3</sub>), 1.85 ppm (s, 6H, Bi-CH<sub>3</sub>). <sup>13</sup>C{<sup>1</sup>H} NMR (125 MHz, CD<sub>2</sub>Cl<sub>2</sub>):  $\delta$  = 27.3 (brs, Bi-CH<sub>3</sub>), 30.01 (s, CNC(CH<sub>3</sub>)<sub>3</sub>), 61.37 (brs, CNC(CH<sub>3</sub>)<sub>3</sub>), 82.52 ppm (brs, CNC(CH<sub>3</sub>)<sub>3</sub>); elemental analysis calcd (%) for [C<sub>7</sub>H<sub>15</sub>NBiSbF<sub>6</sub>] (557.93 g/mol): C 15.07, H 2.71, N 2.51; found: C 14.89, H 2.83, N 2.42. IR (cm<sup>-1</sup>):  $\bar{\nu}$  = 2996 (w, C-H), 2937 (w, C-H), 2242 (w, CN).

**[BiMe<sub>2</sub>(CNAd)(SbF<sub>6</sub>)] (10<sub>Me</sub>):** [BiMe<sub>2</sub>(SbF<sub>6</sub>): 50 mg, 0.11 mmol, 1 equiv.; adamantylisocyanide: 20 mg, 0.12 mmol, 1.1 equiv. During the reaction a colorless precipitate was formed. The crude product was dissolved in dichloromethane (2 mL) and layered with pentane (8 mL). After 18 h the liquid phase was removed and the remaining solid dried in vacuo. Yield: 58 mg (0.09 mmol, 87%) of a colorless solid. <sup>1</sup>H NMR (400 MHz, CD<sub>2</sub>Cl<sub>2</sub>):  $\delta$  = 1.69 (brd, <sup>2</sup>J<sub>H-H</sub> = 13.2 Hz, 3H, H-6<sup>b</sup>, H-8<sup>b</sup>, H-10<sup>b</sup>), 1.74 (br d, <sup>2</sup>J<sub>H-H</sub> = 13.2 Hz, 3H, H-6<sup>a</sup>, H-8<sup>a</sup>, H-10<sup>a</sup>), 1.85 (s, 6H, Bi-CH<sub>3</sub>), 2.13 (d, <sup>3</sup>J<sub>H-H</sub> = 2.8 Hz, 6H, H-2, H-3, H-4), 2.19 ppm (brs, 3H, H-5, H-7, H-9); <sup>13</sup>C{<sup>1</sup>H} NMR (101 MHz, CD<sub>2</sub>Cl<sub>2</sub>):  $\delta$  = 27.5 (brs, CH<sub>3</sub>, Bi-CH<sub>3</sub>), 29.1 (s, CH<sub>2</sub>, C-6, C-8, C-10), 35.2 (s, CH, C-5, C-7, C-9), 42.7 (s, CH<sub>2</sub>, C-2, C-3, C-4), 60.8 (s, C, C-1), 82.43 ppm (brs, C, Isocyanide CNR); <sup>19</sup>F NMR (377 MHz, CD<sub>2</sub>Cl<sub>2</sub>):  $\delta$  = -124.4 ppm (brs, SbF<sub>6</sub>); elemental analysis calcd (%) for [C<sub>13</sub>H<sub>21</sub>NBiSbF<sub>6</sub>] (636.05 g/mol): C 24.55, H 3.33, N 2.20; found: C 24.31, H 3.12, N 2.38. IR (cm<sup>-1</sup>):  $\bar{\nu}$  = 2921 (s, C-H), 2860 (s, C-H), 2229 (w, CN).

**[BiMe<sub>2</sub>(CNXyl)(SbF<sub>6</sub>)] (11<sub>Me</sub>):** [BiMe<sub>2</sub>(SbF<sub>6</sub>): 100 mg, 0.21 mmol, 1 equiv.; 2,6-dimethylphenylisocyanide: 28 mg, 0.21 mmol, 1 equiv. During the reaction a light red precipitate is formed. Yield: 91 mg (0.15 mmol, 71%) of a red solid. <sup>1</sup>H NMR (400 MHz, CD<sub>2</sub>Cl<sub>2</sub>):  $\delta$  = 2.01 (s, 6H, Bi-CH<sub>3</sub>), 2.46 (s, 6H, *ortho*-phenyl CH<sub>3</sub>), 7.24 (d, <sup>3</sup>J<sub>H-H</sub> = 7.6 Hz, 2H, *meta*-phenyl CH), 7.42 ppm (t, <sup>3</sup>J<sub>H-H</sub> = 7.8 Hz, 1 H, *para*-phenyl CH). <sup>13</sup>C{<sup>1</sup>H} NMR (101 MHz, CD<sub>2</sub>Cl<sub>2</sub>):  $\delta$  = 18.8 (s, CH<sub>3</sub>, *ortho*-phenyl CH<sub>3</sub>), 31.0 (brs, Bi-CH<sub>3</sub>), 98.25 (brs, C, isocyanide CNR), 123.4 (brs, C, *ipso*-phenyl C), 129.7 (s, CH, *meta*-phenyl CH), 132.7 (s, CH, *para*-phenyl CH), 137.4 ppm (s, C, *ortho*-phenyl C); elemental analysis calcd (%) for [C<sub>11</sub>H<sub>15</sub>NBiSbF<sub>6</sub>] (605.98 g/mol): C 21.80, H 2.50, N 2.31; found: C 21.42, H 2.22, N 2.41. IR (cm<sup>-1</sup>):  $\bar{\nu}$  = 2928 (w, C-H), 2203 (w, CN), 1590 (m, aromatic ring).

**[BiMe<sub>2</sub>(CNXyl)<sub>2</sub>(SbF<sub>6</sub>)] (11'<sub>Me</sub>):** [BiMe<sub>2</sub>(SbF<sub>6</sub>): 50 mg, 0.11 mmol, 1 equiv.; 2,6-Dimethylphenylisocyanide: 28 mg, 0.21 mmol, 2 equiv. The synthesis was conducted in dichloromethane. During the reaction the solution turned dark red. Yield: 70 mg (0.09 mmol, 90%) of a red-violet solid. <sup>1</sup>H NMR (400 MHz, CD<sub>2</sub>Cl<sub>2</sub>):  $\delta$  = 1.84 (s, 6H, Bi-CH<sub>3</sub>), 2.44 (s, 12H, *ortho*-phenyl CH<sub>3</sub>), 7.20 (d, <sup>3</sup>J<sub>H-H</sub> = 7.6 Hz, 4H, *meta*-phenyl CH), 7.32 ppm (t, <sup>3</sup>J<sub>H-H</sub> = 7.7 Hz, 2H, *para*-phenyl CH); <sup>13</sup>C{<sup>1</sup>H} NMR (101 MHz, CD<sub>2</sub>Cl<sub>2</sub>):  $\delta$  = 18.9 (s, CH<sub>3</sub>, *ortho*-phenyl CH<sub>3</sub>), 24.4 (brs, CH<sub>3</sub>, Bi-CH<sub>3</sub>), 119.76 (brs, C, isocyanide CNR), 125.0 (brs, C, *ipso*-phenyl C), 128.6 (s, CH, *meta*-phenyl CH), 131.1 ppm (s, CH, *para*-phenyl CH), 136.4 (s, C, *ortho*-phenyl C); elemental analysis calcd (%) for [C<sub>20</sub>H<sub>24</sub>N<sub>2</sub>BiSbF<sub>6</sub>] (737.16 g/mol): C 32.59, H 3.28, N 3.80; found: C 32.69, H 3.42, N 3.78. IR (cm<sup>-1</sup>):  $\bar{\nu}$  = 2924 (w, C-H), 2174 (m, CN), 1587 (w, aromatic ring).

**[BiMe<sub>2</sub>(CNCy)(SbF<sub>6</sub>)] (12<sub>Me</sub>):** [BiMe<sub>2</sub>(SbF<sub>6</sub>): 50 mg, 0.11 mmol, 1 equiv.; Cyclohexylisocyanide: 11 mg, 13  $\mu$ L, 0.11 mmol, 1 equiv.

During the reaction the solution turned orange. Yield: 32 mg (0.05 mmol, 52%) of an orange solid. <sup>1</sup>H NMR (400 MHz, CD<sub>2</sub>Cl<sub>2</sub>):  $\delta$  = 1.37–1.58 (brm, 4H, 3,5-Cy CH<sub>2</sub>), 1.63–1.82 (brm, 4H, 2,6-Cy CH<sub>2</sub>), 1.84 (s, 6H, Bi-CH<sub>3</sub>), 1.96–2.07 (brm, 2H, 4-Cy CH<sub>2</sub>), 4.10 ppm (sept, <sup>3</sup>J<sub>H-H</sub> = 4.1 Hz, 1H, 1-Cy CH); <sup>13</sup>C{<sup>1</sup>H} NMR (101 MHz, CD<sub>2</sub>Cl<sub>2</sub>):  $\delta$  = 23.1 (s, CH<sub>2</sub>, 2,6-Cy CH<sub>2</sub>), 24.8 (s, CH<sub>2</sub>, 3,5-Cy CH<sub>2</sub>), 31.1 (brs, CH<sub>3</sub>, Bi-CH<sub>3</sub>), 32.0 (s, CH<sub>2</sub>, 4-Cy CH<sub>2</sub>), 56.2 (s, CH, 1-Cy CH), 84.2 ppm (brs, C, Isocyanide CNR); <sup>19</sup>F NMR (377 MHz, CD<sub>2</sub>Cl<sub>2</sub>):  $\delta$  = -123.2 ppm (brs, SbF<sub>6</sub>); elemental analysis calcd (%) for [C<sub>9</sub>H<sub>17</sub>NBiSbF<sub>6</sub>] (583.97 g/mol): C 18.51, H 2.93, N 2.40; found: C 18.64, H 3.08, N 2.43. IR (cm<sup>-1</sup>):  $\bar{\nu}$  = 2938 (s, C-H), 2861 (s, C-H), 2239 (w, CN).

**[BiMe<sub>2</sub>(CNnBu)(SbF<sub>6</sub>)] (13<sub>Me</sub>):** [BiMe<sub>2</sub>(SbF<sub>6</sub>): 40 mg, 0.08 mmol, 1 equiv.; *n*-butylisocyanide: 7 mg, 9  $\mu$ L, 0.08 mmol, 1 equiv. The synthesis was conducted at 0 °C. Yield: 35 mg (0.06 mmol, 74%) of a dark red oil. <sup>1</sup>H NMR (400 MHz, CD<sub>2</sub>Cl<sub>2</sub>):  $\delta$  = 0.98 (dd, <sup>3</sup>J<sub>H-H</sub> = 7.4 Hz, 3H, H-4), 1.42–1.52 (sext, <sup>3</sup>J<sub>H-H</sub> = 7.5 Hz, 2H, H-3), 1.77–1.84 (quint, <sup>3</sup>J<sub>H-H</sub> = 7.2 Hz, 2H, H-2), 1.89 (s, 6 H, Bi-CH<sub>3</sub>), 3.86 ppm (dd, <sup>3</sup>J<sub>H-H</sub> = 6.6 Hz, 2H, H-1); <sup>13</sup>C{<sup>1</sup>H} NMR (126 MHz, CD<sub>2</sub>Cl<sub>2</sub>):  $\delta$  = 13.2 (s, CH<sub>3</sub>, C-4), 19.8 (s, CH<sub>2</sub>, C-3), 24.1 (s, CH<sub>3</sub>, Bi-CH<sub>3</sub>), 30.5 (s, CH<sub>2</sub>, C-2), 44.11 ppm (brs, CH<sub>2</sub>, C-1);<sup>[1]</sup> elemental analysis calcd (%) for [C<sub>7</sub>H<sub>15</sub>NBiSbF<sub>6</sub>] (557.93 g/mol): C 15.07, H 2.71, N 2.51; found: C 15.35, H 2.844, N 2.57; IR (cm<sup>-1</sup>):  $\bar{\nu}$  = 2965 (s, C-H), 2879 (s, C-H), 2243 (w, CN).<sup>[1]</sup> The signal corresponding to the isocyanide carbon could not be detected due to signal broadening.

## Acknowledgements

Financial support by the DFG (LI2860 5–1) is gratefully acknowledged. This project received funding from the European Research Council (ERC) under the European Union's Horizon 2020 research and innovation program (grant agreement no. 946184). Open Access funding enabled and organized by Projekt DEAL.

## Conflict of Interest

The authors declare no conflict of interest.

## Data Availability Statement

The data that support the findings of this study are available in the supplementary material of this article.

**Keywords:** bismuth · cationic species · Lewis acidity · Lewis pair formation

- [1] C. Lichtenberg, *Chem. Commun.* **2021**, 57, 4483–4495.
- [2] M. Olaru, D. Duvinage, E. Lork, S. Mebs, J. Beckmann, *Angew. Chem. Int. Ed.* **2018**, 57, 10080–10084; *Angew. Chem.* **2018**, 130, 10237–10241.
- [3] M. M. Siddiqui, S. K. Sarkar, M. Nazish, M. Morganti, C. Köhler, J. Cai, L. Zhao, R. Herbst-Irmer, D. Stalke, G. Frenking, H. W. Roesky, *J. Am. Chem. Soc.* **2021**, 143, 1301–1306.
- [4] J. Ramler, A. Stoy, T. Preitschopf, J. Kettner, I. Fischer, B. Roling, F. Fantuzzi, C. Lichtenberg, *Chem. Commun.* **2022**, 58, 9826–9829.
- [5] B. Ritschel, J. Poater, H. Dengel, F. M. Bickelhaupt, C. Lichtenberg, *Angew. Chem. Int. Ed.* **2018**, 57, 3825–3829; *Angew. Chem.* **2018**, 130, 3887–3891.
- [6] K. Oberdorf, P. Grenzer, N. Wieprecht, J. Ramler, A. Hanft, A. Rempel, A. Stoy, K. Radacki, C. Lichtenberg, *Inorg. Chem.* **2021**, 60, 19086–19097.

- [7] B. Ritschel, C. Lichtenberg, *Synlett* **2018**, 29, 2213–2217.
- [8] J. Ramler, F. Fantuzzi, F. Geist, A. Hanft, H. Braunschweig, B. Engels, C. Lichtenberg, *Angew. Chem. Int. Ed.* **2021**, 60, 24388–24394; *Angew. Chem.* **2021**, 133, 24592–24598.
- [9] J. E. Walley, L. S. Warring, G. Wang, D. A. Dickie, S. Pan, G. Frenking, R. J. Gilliard, *Angew. Chem. Int. Ed.* **2021**, 60, 6682–6690; *Angew. Chem.* **2021**, 133, 6756–6764.
- [10] a) J. Ramler, J. Poater, F. Hirsch, B. Ritschel, I. Fischer, F. M. Bickelhaupt, C. Lichtenberg, *Chem. Sci.* **2019**, 10, 4169–4176; b) A. Hanft, K. Radacki, C. Lichtenberg, *Chem. Eur. J.* **2021**, 27, 6230–6239.
- [11] For a rare case of reversible one-electron transfer at bismuth, starting from a neutral bismuth compound, see: H. M. Weinert, C. Wölper, J. Haak, G. E. Cutsail, S. Schulz, *Chem. Sci.* **2021**, 12, 14024–14032.
- [12] C. Lichtenberg, F. Pan, T. P. Spaniol, U. Englert, J. Okuda, *Angew. Chem. Int. Ed.* **2012**, 51, 13011–13015; *Angew. Chem.* **2012**, 124, 13186–13190.
- [13] S. Balasubramaniam, S. Kumar, A. P. Andrews, B. Varghese, E. D. Jemmis, A. Venugopal, *Eur. J. Inorg. Chem.* **2019**, 2019, 3265–3269.
- [14] R. Kannan, S. Balasubramaniam, S. Kumar, R. Chambenahalli, E. D. Jemmis, A. Venugopal, *Chem. Eur. J.* **2020**, 26, 12717–12721.
- [15] a) O. Planas, V. Peciukenas, J. Cornella, *J. Am. Chem. Soc.* **2020**, 142, 11382–11387; b) O. Planas, F. Wang, M. Leutzsch, J. Cornella, *Science* **2020**, 367, 313–317.
- [16] W. Frank, G. J. Reiss, J. Schneider, *Angew. Chem. Int. Ed.* **1995**, 34, 2416–2417; *Angew. Chem.* **1995**, 107, 2572–2573.
- [17] J. Ramler, C. Lichtenberg, *Chem. Eur. J.* **2020**, 26, 10250–10258.
- [18] R. Kannan, S. Kumar, A. P. Andrews, E. D. Jemmis, A. Venugopal, *Inorg. Chem.* **2017**, 56, 9391–9395.
- [19] L. S. Warring, J. E. Walley, D. A. Dickie, W. Tiznado, S. Pan, R. J. Gilliard, *Inorg. Chem.* **2022**, 61, 18640–18652.
- [20] a) I. M. Riddlestone, A. Kraft, J. Schaefer, I. Krossing, *Angew. Chem. Int. Ed.* **2018**, 57, 13982–14024; *Angew. Chem.* **2018**, 130, 14178–14221; b) I. Krossing, I. Raabe, *Angew. Chem. Int. Ed.* **2004**, 43, 2066–2090; *Angew. Chem.* **2004**, 116, 2116–2142; c) T. A. Engesser, M. R. Lichtenhaler, M. Schleep, I. Krossing, *Chem. Soc. Rev.* **2016**, 45, 789–899.
- [21] H. Dengel, C. Lichtenberg, *Chem. Eur. J.* **2016**, 22, 18465–18475.
- [22] S. Solyntjes, J. Bader, B. Neumann, H.-G. Stammler, N. Ignat'ev, B. Hoge, *Chem. Eur. J.* **2017**, 23, 1557–1567.
- [23] J. Kuziola, M. Magre, N. Nöthling, J. Cornella, *Organometallics* **2022**, 41, 1754–1762.
- [24] a) S. Solyntjes, B. Neumann, H.-G. Stammler, N. Ignat'ev, B. Hoge, *Eur. J. Inorg. Chem.* **2016**, 2016, 3999–4010; b) A. Schmuck, D. Leopold, S. Wallenhauer, K. Seppelt, *Chem. Ber.* **1990**, 123, 761–766.
- [25] C. J. Carmalt, L. J. Farrugia, N. C. Norman, *J. Chem. Soc. Dalton Trans.* **1996**, 443.
- [26] D. Duvinage, L. A. Malaspina, S. Grabowsky, S. Mebs, J. Beckmann, *Eur. J. Inorg. Chem.* **2023**, 26, e202200482.
- [27] P. Erdmann, J. Leitner, J. Schwarz, L. Greb, *ChemPhysChem* **2020**, 21, 987–994.
- [28] A.-M. Preda, M. Krasowska, L. Wrobel, P. Kitschke, P. C. Andrews, J. G. MacLellan, L. Mertens, M. Korb, T. Rüffer, H. Lang, A. A. Auer, M. Mehrling, *Beilstein J. Org. Chem.* **2018**, 14, 2125–2145.
- [29] H. J. Breunig, E. Lork, C. Rat, *Z. Naturforsch. B* **2007**, 62, 1224–1226.
- [30] M. Mantina, A. C. Chamberlin, R. Valero, C. J. Cramer, D. G. Truhlar, *J. Phys. Chem. A* **2009**, 113, 5806–5812.
- [31] A. Bondi, *J. Phys. Chem.* **1964**, 68, 441–451.
- [32] T. Dunaj, K. Dollberg, C. Ritter, F. Dankert, C. Hänisch, *Eur. J. Inorg. Chem.* **2021**, 2021, 870–878.
- [33] U. Mayer, V. Gutmann, W. Gerger, *Monatsh. Chem.* **1975**, 106, 1235–1257.
- [34] M. A. Beckett, G. C. Strickland, J. R. Holland, K. Sukumar Varma, *Polymer* **1996**, 37, 4629–4631.
- [35] a) H. J. Breunig, K. H. Ebert, R. E. Schulz, M. Wieber, I. Sauer, *Z. Naturforsch. B* **1995**, 50, 735–744; b) G. G. Briand, A. Decken, N. M. Hunter, G. M. Lee, J. A. Melanson, E. M. Owen, *Polyhedron* **2012**, 31, 796–800.
- [36] a) L. Greb, *Chem. Eur. J.* **2018**, 24, 17881–17896; b) P. Erdmann, L. Greb, *Angew. Chem. Int. Ed.* **2022**, 61, e202114550.
- [37] J. Ramler, K. Hofmann, C. Lichtenberg, *Inorg. Chem.* **2020**, 59, 3367–3376.
- [38] M. Giustiniano, A. Basso, V. Mercalli, A. Massarotti, E. Novellino, G. C. Tron, J. Zhu, *Chem. Soc. Rev.* **2017**, 46, 1295–1357.
- [39] S. Mukhopadhyay, A. G. Patro, R. S. Vadavi, S. Nembenna, *Eur. J. Inorg. Chem.* **2022**, e202200469.
- [40] W. Lu, H. Hu, Y. Li, R. Ganguly, R. Kinjo, *J. Am. Chem. Soc.* **2016**, 138, 6650–6661.
- [41] M. Seidl, M. Schiffer, M. Bodensteiner, A. Y. Timoshkin, M. Scheer, *Chem. Eur. J.* **2013**, 19, 13783–13791.
- [42] R. W. Stephany, M. J. A. de Bie, W. Drenth, *Org. Magn. Reson.* **1974**, 6, 45–47.
- [43] a) A. Aprile, R. Corbo, K. Vin Tan, D. J. D. Wilson, J. L. Dutton, *Dalton Trans.* **2014**, 43, 764–768; b) J. B. Waters, Q. Chen, T. A. Everitt, J. M. Goicoechea, *Dalton Trans.* **2017**, 46, 12053–12066; c) J. E. Walley, L. S. Warring, E. Kertész, G. Wang, D. A. Dickie, Z. Benkő, R. J. Gilliard, *Inorg. Chem.* **2021**, 60, 4733–4743; d) G. Wang, L. A. Freeman, D. A. Dickie, R. Mokrai, Z. Benkő, R. J. Gilliard, *Chem. Eur. J.* **2019**, 25, 4335–4339; e) G. Wang, L. A. Freeman, D. A. Dickie, R. Mokrai, Z. Benkő, R. J. Gilliard, *Inorg. Chem.* **2018**, 57, 11687–11695; f) R. Deka, A. Orthaber, *Dalton Trans.* **2022**, 51, 8540–8556.
- [44] a) G. M. Sheldrick, *Acta Crystallogr. Sect. A* **2015**, 71, 3–8; b) G. M. Sheldrick, *Acta Crystallogr. Sect. A* **2008**, 64, 112–122.
- [45] It should be noted that neutral bismuth species have also found use in remarkable transformations such as small molecule activation, CH activation, radical dehydrocoupling, and cyclo-isomerization reactions, for example: a) M. Magre, J. Cornella, *J. Am. Chem. Soc.* **2021**, 143, 21497–21502; b) S. Roggan, C. Limberg, B. Ziemer, M. Brandt, *Angew. Chem. Int. Ed.* **2004**, 43, 2846–2849; *Angew. Chem.* **2004**, 116, 2906–2910; c) S. Roggan, G. Schnakenburg, C. Limberg, S. Sandhöfner, H. Pritzkow, B. Ziemer, *Chem. Eur. J.* **2005**, 11, 225–234; d) R. J. Schwamm, M. Lein, M. P. Coles, C. M. Fitchett, *Angew. Chem. Int. Ed.* **2016**, 55, 14798–14801; *Angew. Chem.* **2016**, 128, 15018–15021; e) R. J. Schwamm, M. Lein, M. P. Coles, C. M. Fitchett, *J. Am. Chem. Soc.* **2017**, 139, 16490–16493; f) J. Ramler, I. Krummenacher, C. Lichtenberg, *Angew. Chem. Int. Ed.* **2019**, 58, 12924–12929; *Angew. Chem.* **2019**, 131, 13056–13062; g) K. Oberdorf, A. Hanft, J. Ramler, I. Krummenacher, M. Bickelhaupt, J. Poater, C. Lichtenberg, *Angew. Chem. Int. Ed.* **2021**, 60, 6441–6445; *Angew. Chem.* **2021**, 133, 6513–6518; h) J. Ramler, I. Krummenacher, C. Lichtenberg, *Chem. Eur. J.* **2020**, 26, 14551–14555; i) J. Ramler, J. Schwarzmann, A. Stoy, C. Lichtenberg, *Eur. J. Inorg. Chem.* **2022**, e202100934; j) X. Yang, E. Reijerse, K. Bhattacharyya, M. Leutzsch, M. Kochius, N. Nöthling, J. Busch, A. Schnegg, A. Auer, J. Cornella, *J. Am. Chem. Soc.* **2022**, 144, 16535–16544; k) D. R. Kindra, I. J. Casely, M. E. Fieser, J. W. Ziller, F. Furche, W. J. Evans, *J. Am. Chem. Soc.* **2013**, 135, 7777–7787.

Manuscript received: December 22, 2022  
Accepted manuscript online: March 8, 2023  
Version of record online: March 31, 2023